USDA FOREST SERVICE
RESEARCH PAPER
FPL 156
1972

DESIGN PARAMETERS FOR TORSION OF SANDWICH STRIPS HAVING TRAPEZOIDAL, RECTANGULAR, AND TRIANGULAR CROSS SECTIONS

FOREST PRODUCTS LABORATORY, FOREST SERVICE
U.S. DEPARTMENT OF AGRICULTURE, MADISON, WIS.

THIS REPORT IS ONE OF A SERIES
ISSUED IN COOPERATION WITH THE
MIL-HDBK-23 WORKING GROUP ON STRUCTURAL SANDWICH COMPOSITES
FOR AEROSPACE VEHICLES
OF THE DEPARTMENTS OF THE
AIR FORCE AND NAVY, AND FEDERAL AVIATION ADMINISTRATION

Abstract

Solutions for the elastic torsion of sandwich strips having triangular, rectangular, or trapezoidal cross sections are presented analytically in terms of suitable design parameters. Data obtained from resulting expressions are presented in a series of design curves for normalized values of torsional stiffness and maximum facing and core shear stresses.

The analysis is based on the Saint Venant theory of torsion. The sandwich facings are idealized as identical, thin, isotropic membranes, while the core's elastic behavior is characterized by a single transverse modulus of rigidity.

The U.S. Forest Products Laboratory
is maintained at Madison, Wis.,
in cooperation with the
University of Wisconsin

DESIGN PARAMETERS FOR TORSION OF SANDWICH STRIPS HAVING TRAPEZOIDAL, RECTANGULAR, AND TRIANGULAR CROSS SECTIONS[1]

By

H. M. MONTREY, Engineer
and
EDWARD W. KUENZI, Engineer

Forest Products Laboratory, Forest Service
U.S. Department of Agriculture

Introduction

Structural sandwich composites in aircraft construction are frequently loaded in torsion. To aid in the design of such flight vehicle components, solutions are derived and presented herein for the elastic torsion of sandwich strips having various cross sections. Explicit expressions for the torsional stiffness, maximum facing shear stress, and maximum core shear stress are developed and presented both analytically and as a series of design curves for normalized values of these quantities.

The theory and governing equations used are taken from an earlier work by Cheng, [2] which expanded on a previous work by the same author. [3] The analysis is based on the Saint Venant theory of torsion, the details of which are provided by Timoshenko and Goodier. [4] The facings are assumed to be thin isotropic membranes of equal thickness, while core stiffnesses are assumed negligible in all directions except that normal to the sandwich.

Numerical results for trapezoidal sections are shown to converge to results for rectangular sections in the proper limit. Furthermore, certain results for rectangular sections are shown to reduce to the predictions of an elementary analysis for torsion of hollow, thin-walled sections.

---

[1] This report is another in a series issued in cooperation with the Military Handbook 23 Working Group on Structural Sandwich Composites for Aerospace Vehicles of the Departments of the Air Force and Navy, and Federal Aviation Administration under DO F33-615-72-M-5001.

[2] Cheng, S. Torsion of Sandwich Panels of Trapezoidal, Triangular, and Rectangular Cross Sections. Forest Products Lab. Rep. 1874. 1960.

[3] Cheng, S. Torsion of Rectangular Sandwich Plates. Forest Products Lab. Rep. 1871. 1959.

[4] Timoshenko, S., and Goodier, J. N. Theory of Elasticity. McGraw-Hill, N.Y. 1951.

Notation

x, y, z	Cartesian coordinates for core
x_1, y_1, z_1	Cartesian coordinates for facings
h	Minimum distance separating facing midplanes
b	Plate width
L	Plate length
t	Facing thickness
G	Facing modulus of rigidity
G_c	Core modulus of rigidity
θ	Angle of twist
T	Applied torque
α	Angle of slope of facings
τ	Facing shear stress
τ_c	Core shear stress
ω	$\frac{G_c}{tG\cos\alpha\tan^2\alpha}$
γ	$\frac{2hG_c}{tG(h+t)^2}$
β	$\frac{G_c}{tG\sin\alpha}$
V	$\frac{thG}{2b^2G_c}$
R	$\frac{\tan\alpha}{h/b}$
W	$\frac{tG}{2bG_c}$
k_1	Normalized torsional stiffness
k_2	Normalized maximum facing shear stress
k_3	Normalized maximum core shear stress
I_ν, K_ν	Modified Bessel functions of the first and second kind, respectively, and of order ν

Theoretical Development

1. Assumptions

The primary assumption invoked is that of the Saint Venant theory for torsion of prismatical bodies, which specifies that the distribution of shear stresses is the same on all sections normal to the axis of twist.

The facings are taken to be identical, thin, uniform membranes of an isotropic material. The core in-plane stiffnesses parallel to the facings are assumed to be negligibly small (as is the case with all honeycomb cores). As a consequence, there remains only one nonvanishing core shear stress which is constant throughout the thickness of the core.

Shear stress in the facings is forced to vanish at free edges of the sandwich.

2. Governing Differential Equations

The differential equations follow for the shear stress components within the core and the facings during torsion of the sandwich strip. The notation used is for the most part that used by Cheng,[2] and the differential equations are due to his derivations.

Trapezoidal sections.--A sandwich strip with a symmetrical trapezoidal cross section is shown in figure 1. In the figure, the xy plane is taken to be the mid-plane of the core, and the x_1y_1 plane is the plane of the top (or bottom, if desired) facing. The z and z_1 axes are chosen as normal to core midplane and facing, respectively, and α denotes the angular orientation of the facing relative to that of the core midplane. Using this notation,

$$z = \frac{h}{2} + y\tan\alpha \tag{1}$$

where h is the minimum distance separating the two facing middle surfaces.

If the sandwich length L is sufficiently large, the stresses and strains during torsion can be assumed not to vary along the longitudinal axis of twist, according to Saint Venant. Utilizing this assumption, Cheng[2] has derived the governing differential equation for the facing shear stress $\tau_{y_1z_1}$ (subsequently denoted as τ) for torsion about the x axis. For thin facings, this equation becomes

$$z\frac{d^2\tau}{dz^2} + \frac{d\tau}{dz} - \omega\tau = \frac{-2G_c}{t\tan^2\alpha}\frac{\theta}{L}z \tag{2}$$

where G_c represents the core modulus of rigidity in the xz plane, t the facing thickness, and θ the total plate angle of twist. Also,

$$\omega = \frac{G_c}{tG\cos\alpha\tan^2\alpha} \tag{3}$$

where G is the facing modulus of rigidity.

Cheng also found the nonvanishing core shear stress τ_{xz} (subsequently denoted as τ_c) to be given by

$$\tau_c = t\left(1 + \frac{t\cos\alpha}{2z}\right)\frac{d\tau}{dy} \tag{4}$$

The problem of completely determining the stress state in the facings and core reduces to that of finding the solution of equation (2), subject to the condition that τ must vanish at the free edges y = 0 and y = b (b being the sandwich width), and then applying equation (4).

Rectangular sections.--A sandwich strip with a rectangular cross section is shown in figure 2. The governing differential equation for the facing shear stress τ is obtained by forcing α to vanish in equation (2), yielding

$$\frac{d^2\tau}{dy^2} - \gamma^2\tau = \frac{-4hG_c}{t(h + t)}\frac{\theta}{L} \tag{5}$$

where

$$\gamma^2 = \frac{2hG_c}{tG(h + t)^2} \tag{6}$$

The core shear stress τ_c can be similarly obtained from equation (4) as

$$\tau_c = \frac{t(h + t)}{h}\frac{d\tau}{dy} \tag{7}$$

The complete stress state in the core and facings is obtained by solving equation (5) subject to the conditions $\tau = 0$ at y = 0 and y = b, and by utilizing equation (7).

Triangular sections.--A sandwich strip with a triangular cross section is shown in figure 3. The governing differential equation for the facing shear stress τ is obtained by forcing h to vanish in equation (2), yielding

$$y\frac{d^2\tau}{dy^2} + \frac{d\tau}{dy} - \beta\tau = \frac{-2G_c}{t}\frac{\theta}{L}y \tag{8}$$

where

$$\beta = \frac{G_c}{tG\sin\alpha} \tag{9}$$

and similarly, from equation (4), the core shear stress τ_c becomes

$$\tau_c = t\left(1 + \frac{t\cos^2\alpha}{2y\sin\alpha}\right)\frac{d\tau}{dy} \tag{10}$$

As with the trapezoidal and rectangular sections, the facing shear stress τ for this section must vanish at the edge y = b. However, since the corner y = 0 is not a free edge, and since the shear stress in the top and bottom facings must be equal there, τ is required only to be bounded in magnitude at y = 0.

3. Analytical Solutions

Expressions follow for the facing shear stress, core shear stress, and torsional stiffness for torsion of sandwich strips having each of the three sections under consideration.

Trapezoidal sections.--The general solution for the facing shear stress τ, satisfying equation (2), is given by Cheng [2] as

$$\frac{\tau}{\theta/L} = 2G\cos\alpha\left(z + \frac{1}{\omega}\right) + C_1 I_0(2\sqrt{\omega z}) + C_2 K_0(2\sqrt{\omega z}) \tag{11}$$

where I_0 and K_0 represent modified Bessel functions of the first and second kind, respectively, and of order zero, and C_1 and C_2 are constants determined by application of the stress boundary conditions.

The shear stress τ must vanish at the edges y = 0 and y = b, from which, with the aid of equation (1),

$$\frac{C_1}{2G\cos\alpha} = \frac{\begin{vmatrix} K_0(\sqrt{2\omega h}) & \frac{h}{2} + \frac{1}{\omega} \\ K_0\left(2\sqrt{\omega\left(\frac{h}{2} + b\tan\alpha\right)}\right) & \frac{h}{2} + b\tan\alpha + \frac{1}{\omega} \end{vmatrix}}{\begin{vmatrix} I_0(\sqrt{2\omega h}) & K_0(\sqrt{2\omega h}) \\ I_0\left(2\sqrt{\omega\left(\frac{h}{2} + b\tan\alpha\right)}\right) & K_0\left(2\sqrt{\omega\left(\frac{h}{2} + b\tan\alpha\right)}\right) \end{vmatrix}} \tag{12}$$

$$\frac{C_2}{2G\cos\alpha} = \frac{\begin{vmatrix} \frac{h}{2} + \frac{1}{\omega} & I_0(\sqrt{2\omega h}) \\ \frac{h}{2} + b\tan\alpha + \frac{1}{\omega} & I_0\left(2\sqrt{\omega\left(\frac{h}{2} + b\tan\alpha\right)}\right) \end{vmatrix}}{\begin{vmatrix} I_0(\sqrt{2\omega h}) & K_0(\sqrt{2\omega h}) \\ I_0\left(2\sqrt{\omega\left(\frac{h}{2} + b\tan\alpha\right)}\right) & K_0\left(2\sqrt{\omega\left(\frac{h}{2} + b\tan\alpha\right)}\right) \end{vmatrix}}$$

The core shear stress τ_c can be found by combining equations (4) and (11) and is of the form

$$\frac{\tau_c}{\theta/L} = t\left(1 + \frac{t\cos\alpha}{2z}\right)\tan\alpha\left[2G\cos\alpha + C_1\sqrt{\frac{\omega}{z}}\,I_1\left(2\sqrt{\omega z}\right) - C_2\sqrt{\frac{\omega}{z}}\,K_1\left(2\sqrt{\omega z}\right)\right] \tag{13}$$

The relationship between the externally applied torque T and the facing shear stress τ is documented by Cheng [2] as

$$T = 4t\int_0^b \tau z\,dy + \frac{t^2(1 + \cos^2\alpha)}{\cos\alpha}\int_0^b \tau\,dy \tag{14}$$

Combining equations (11) and (14) yields, after considerable integration and simplification, the torsional stiffness of the sandwich. In particular,

$$\begin{aligned}\frac{T}{\theta/L} = {} & \left\langle \frac{2tG\cos\alpha}{\tan\alpha}\left[4\left(\frac{z^3}{3} + \frac{z^2}{2\omega}\right) + \frac{t(1 + \cos^2\alpha)}{\cos\alpha}\left(\frac{z^2}{2} + \frac{z}{\omega}\right)\right]\right. \\ & + \frac{4t}{\omega^2\tan\alpha}\left\{C_1\left[\sqrt{\omega z}\,(\omega z + 1)I_1\left(2\sqrt{\omega z}\right) - \omega z I_0\left(2\sqrt{\omega z}\right)\right]\right. \\ & \left. - C_2\left[\sqrt{\omega z}\,(\omega z + 1)K_1\left(2\sqrt{\omega z}\right) + \omega z K_0\left(2\sqrt{\omega z}\right)\right]\right\} \\ & \left. + \frac{t^2\sqrt{\omega z}\,(1 + \cos^2\alpha)}{\omega\tan\alpha\cos\alpha}\left[C_1 I_1\left(2\sqrt{\omega z}\right) - C_2 K_1\left(2\sqrt{\omega z}\right)\right]\right\rangle \Bigg|_{\frac{h}{2}}^{\frac{h}{2} + b\tan\alpha}\end{aligned} \tag{15}$$

where C_1 and C_2 are given by equations (12). Equations (15), (11), and (13) give the torsional stiffness, facing shear stress, and core shear stress, respectively, for torsion of a sandwich strip having a trapezoidal cross section.

Rectangular sections.--The general solution for the facing shear stress τ, satisfying equation (5), is given by Cheng [2] as

$$\frac{\tau}{\theta/L} = G(h + t) + B_1\sinh\gamma y + B_2\cosh\gamma y \tag{16}$$

The constants B_1 and B_2 are determined by applying the boundary conditions $\tau = 0$ at $y = 0$ and $y = b$. After applying these conditions, equation (16) becomes

$$\frac{\tau}{\theta/L} = G(h + t)\left\{\frac{\cosh\gamma b - 1}{\sinh\gamma b}\sinh\gamma y - \cosh\gamma y + 1\right\} \tag{17}$$

Combining equations (7) and (17) yields τ_c to be of the form

$$\frac{\tau_c}{\theta/L} = G(h + t)\sqrt{\frac{2tG_c}{hG}}\left\{\frac{\cosh\gamma b - 1}{\sinh\gamma b}\cosh\gamma y - \sinh\gamma y\right\} \tag{18}$$

The externally applied torque T is related to the facing and core shear stresses by

$$T = t(h + t)\int_0^b \tau dy - h\int_0^b \tau_c dy \tag{19}$$

Combining equations (17), (18), and (19) yields

$$\frac{T}{\theta/L} = 2t(h + t)^2 Gb\left[1 - \frac{2(\cosh\gamma b - 1)}{\gamma b\sinh\gamma b}\right] \tag{20}$$

Equations (20), (17), and (18) give the torsional stiffness, facing shear stress, and core shear stress, respectively, for torsion of a sandwich strip having a rectangular cross section.

Triangular sections.--The general solution for the facing shear stress τ, satisfying equation (8), can be shown to be

$$\frac{\tau}{\theta/L} = 2G\sin\alpha\left(y + \frac{1}{\beta}\right) + A_1 I_0(2\sqrt{\beta y}) + A_2 K_0(2\sqrt{\beta y}) \tag{21}$$

The constants A_1 and A_2 are determined as follows: Since τ must have some finite value at the corner $y = 0$, the constant A_2 must vanish, Applying this and the condition $\tau = 0$ at $y = b$ yields

$$\frac{\tau}{\theta/L} = 2G\sin\alpha\left\{y + \frac{1}{\beta} - \left(b + \frac{1}{\beta}\right)\frac{I_0(2\sqrt{\beta y})}{I_0(2\sqrt{\beta b})}\right\} \tag{22}$$

Applying equation (10) yields the core shear stress as

$$\frac{\tau_c}{\theta/L} = 2tG\sin\alpha\left(1 + \frac{t\cos^2\alpha}{2y\sin\alpha}\right)\left\{1 - \sqrt{\frac{\beta}{y}}\left(b + \frac{1}{\beta}\right)\frac{I_1(2\sqrt{\beta y})}{I_0(2\sqrt{\beta b})}\right\} \tag{23}$$

Forcing h to vanish in equation (14) yields the relationship between the torque T and the facing shear stress τ:

$$T = 4t \tan\alpha \int_0^b \tau y dy + \frac{t^2(1 + \cos^2\alpha)}{\cos\alpha} \int_0^b \tau dy \tag{24}$$

Combining equations (22) and (24) yields, after considerable integration and simplification,

$$\begin{aligned} \frac{T}{\theta/L} = {} & 8tG\sin\alpha\tan\alpha \left\{ \frac{b^3}{3} + \frac{b^2}{2\beta} - \frac{b + 1/\beta}{I_0(2\sqrt{\beta}b)} \left[\frac{b^2}{\sqrt{\beta}b} I_1(2\sqrt{\beta}b) - \frac{b}{\beta} I_2(2\sqrt{\beta}b) \right] \right\} \\ & + 2t^2 G\tan\alpha(1 + \cos^2\alpha) \left\{ \frac{b^2}{2} + \frac{b}{\beta} - \frac{b + 1/\beta}{I_0(2\sqrt{\beta}b)} \left[\frac{b}{\sqrt{\beta}b} I_1(2\sqrt{\beta}b) \right] \right\} \end{aligned} \tag{25}$$

Equations (25), (22), and (23) give the torsional stiffness and facing and core shear stresses, respectively, for torsion of a sandwich strip having a triangular cross section.

4. Design Parameters for Stiffness and Maximum Stresses

The quantities of primary interest to design engineers and other technical personnel are those giving measures of stiffness and maximum stress levels. For the problem under consideration here, the quantities of interest are the torsional stiffness $\frac{T}{\theta/L}$, and maximum values of the facing shear stress τ, and the core shear stress τ_c.

To provide means of presenting these desired data, definitions follow for suitable design parameters. Detailed derivations for the desired quantities are then presented in terms of these design parameters.

Rectangular and trapezoidal sections.--Introduce the shear parameter V defined by

$$V = \frac{thG}{2b^2 G_c} \tag{26}$$

Upon making this substitution, it becomes possible to write equation (20), for rectangular sections, into the form

$$\frac{T}{\theta/L} = \frac{2th^2 bG}{k_1(\text{RECT})} \tag{27}$$

where

$$\frac{1}{k_1^{(RECT)}} = 1 - 2\sqrt{V}\tanh\frac{1}{2\sqrt{V}} \tag{28}$$

Since $\frac{t}{h} << 1$ for thin facings, terms involving this quantity are neglected in this and all subsequent derivations.

Utilizing this definition of $\underline{V}$, it becomes possible, after considerable simplification, to also write equation (15), for trapezoidal sections, into the form

$$\frac{T}{\theta/L} = \frac{2th^2bG}{k_1^{(TRAP)}} \tag{29}$$

where

$$\begin{aligned}\frac{1}{k_1^{(TRAP)}} = {} & \cos\alpha + 2\left(\frac{b}{h}\right)\cos\alpha\tan\alpha + \frac{4}{3}\left(\frac{b}{h}\right)^2\cos\alpha\tan^2\alpha + 4V\left(\frac{b}{h}\right)^2\cos^2\alpha\tan^2\alpha \\ & + 4V\left(\frac{b}{h}\right)^3\cos^2\alpha\tan^3\alpha + 8V^2\cos^3\alpha\tan^3\alpha\left(\frac{b}{h}\right)^3\left\{\xi\left[\frac{\phi}{2}\left(\frac{\phi^2}{4}+1\right)I_1(\phi)\right.\right. \\ & \left. - \frac{\psi}{2}\left(\frac{\psi^2}{4}+1\right)I_1(\psi) - \frac{\phi^2}{4}I_0(\phi) + \frac{\psi^2}{4}I_0(\psi)\right] - \eta\left[\frac{\phi}{2}\left(\frac{\phi^2}{4}+1\right)K_1(\phi)\right. \\ & \left.\left. - \frac{\psi}{2}\left(\frac{\psi^2}{4}+1\right)K_1(\psi) + \frac{\phi^2}{4}K_0(\phi) - \frac{\psi^2}{4}K_0(\psi)\right]\right\}\end{aligned} \tag{30}$$

in which

$$\begin{aligned}\xi &= \frac{\left[1 + 2\left(\frac{b}{h}\right)\tan\alpha + 4V\left(\frac{b}{h}\right)^2\cos\alpha\tan^2\alpha\right]K_0(\psi) - \left[1 + 4V\left(\frac{b}{h}\right)^2\cos\alpha\tan^2\alpha\right]K_0(\phi)}{I_0(\psi)K_0(\phi) - I_0(\phi)K_0(\psi)} \\ \eta &= \frac{\left[1 + 4V\left(\frac{b}{h}\right)^2\cos\alpha\tan^2\alpha\right]I_0(\phi) - \left[1 + 2\left(\frac{b}{h}\right)\tan\alpha + 4V\left(\frac{b}{h}\right)^2\cos\alpha\tan^2\alpha\right]I_0(\psi)}{I_0(\psi)K_0(\phi) - I_0(\phi)K_0(\psi)}\end{aligned} \tag{31}$$

and

$$\phi = \sqrt{\frac{\left(\frac{h}{b}\right)^2 + 2\left(\frac{h}{b}\right)\tan\alpha}{V\cos\alpha\tan^2\alpha}}$$

$$\psi = \sqrt{\frac{\left(\frac{h}{b}\right)^2}{V\cos\alpha\tan^2\alpha}} \qquad (32)$$

To determine the maximum value of the facing shear stress τ in rectangular sections, first rewrite equation (17) into the form

$$\tau = \frac{Gh\theta}{L}\left\{\left(\frac{\cosh\frac{1}{\sqrt{V}} - 1}{\sinh\frac{1}{\sqrt{V}}}\right)\sinh\frac{1}{\sqrt{V}}\frac{y}{b} - \cosh\frac{1}{\sqrt{V}}\frac{y}{b} + 1\right\} \qquad (33)$$

Differentiating equation (33) with respect to y/b and setting the result equal to zero yields the location of the maximum facing shear stress. In particular

$$\tanh\frac{1}{\sqrt{V}}\frac{y}{b} = \frac{\cosh\frac{1}{\sqrt{V}} - 1}{\sinh\frac{1}{\sqrt{V}}} = \tanh\frac{1}{2\sqrt{V}}$$

from which y = b/2 is found to maximize τ. Substituting this result into equation (29) and simplifying yields the maximum facing shear stress τ_{MAX}:

$$\tau_{MAX} = \frac{T}{2thb}k_2^{(RECT)} \qquad (34)$$

where

$$k_2^{(RECT)} = k_1^{(RECT)}\left\{1 - \operatorname{sech}\frac{1}{2\sqrt{V}}\right\} \qquad (35)$$

To determine the maximum facing shear stress in trapezoidal sections, differentiate τ as given by equations (11) and (12) and utilize equation (26), yielding

$$\eta K_1\left[\frac{h}{b}\sqrt{\frac{1+2\left(\frac{b}{h}\right)\left(\frac{y}{b}\right)\tan\alpha}{V\cos\alpha\tan^2\alpha}}\right]-\xi I_1\left[\frac{h}{b}\sqrt{\frac{1+2\left(\frac{b}{h}\right)\left(\frac{y}{b}\right)\tan\alpha}{V\cos\alpha\tan^2\alpha}}\right]$$

$$=2\left(\frac{b}{h}\right)\tan\alpha\sqrt{V\cos\alpha\left[1+2\left(\frac{b}{h}\right)\left(\frac{y}{b}\right)\tan\alpha\right]} \tag{36}$$

The maximum facing shear stress τ_{MAX} can then be written in the same form as for rectangular sections:

$$\tau_{MAX}=\frac{T}{2thb}k_2^{(TRAP)} \tag{37}$$

where

$$k_2^{(TRAP)}=k_1^{(TRAP)}\cos\alpha\left\{1+2\left(\frac{b}{h}\right)\left(\frac{y}{b}\right)\tan\alpha+4V\left(\frac{b}{h}\right)^2\cos\alpha\tan^2\alpha\right.$$

$$\left.+\xi I_0\left[\frac{h}{b}\sqrt{\frac{1+2\left(\frac{b}{h}\right)\left(\frac{y}{b}\right)\tan\alpha}{V\cos\alpha\tan^2\alpha}}\right]+\eta K_0\left[\frac{h}{b}\sqrt{\frac{1+2\left(\frac{b}{h}\right)\left(\frac{y}{b}\right)\tan\alpha}{V\cos\alpha\tan^2\alpha}}\right]\right\} \tag{38}$$

with y/b being the solution of equation (36).

To determine the maximum value of the core shear stress τ_c in rectangular sections, first rewrite equation (18) into the form

$$\tau_c=\sqrt{\frac{2G_c}{thG}}\frac{tGh\theta}{L}\left\{\frac{\cosh\frac{1}{2\sqrt{V}}-1}{\sinh\frac{1}{2\sqrt{V}}}\cosh\frac{1}{\sqrt{V}}\frac{y}{b}-\sinh\frac{1}{\sqrt{V}}\frac{y}{b}\right\} \tag{39}$$

Differentiating equation (39) with respect to y/b and forcing the result to vanish yields an equation for y/b having only imaginary roots, implying no absolute maximum for τ_c in the range $0 \leq y \leq b$. In fact, τ_c as given by equation (32) is a smoothly decreasing function of y/b with relative maximum and minimum at $y = 0$ and $y = b$, respectively. Furthermore, these extrema have identical absolute values. Choosing $y = 0$, it becomes possible to present the maximum core shear stress in the form

$$\tau_{c_{MAX}}=\frac{T}{2hb}\sqrt{\frac{2G_c}{thG}}k_3^{(RECT)} \tag{40}$$

where

$$k_3^{(RECT)} = k_1^{(RECT)} \tanh \frac{1}{2\sqrt{V}} \tag{41}$$

The maximum core shear stress in trapezoidal sections is determined in the same manner. From equation (13), the maximum value of τ_c can be written in the same form as for rectangular sections:

$$\tau_{c_{MAX}} = \frac{T}{2hb} \sqrt{\frac{2G_c}{thG}}\, k_3^{(TRAP)} \tag{42}$$

where

$$k_3^{(TRAP)} = k_1^{(TRAP)} \sqrt{V} \left(\frac{b}{h}\right) \cos\alpha\tan\alpha \left\langle 2 + \frac{\frac{h}{b}}{\sqrt{V\cos\alpha\tan^2\alpha\left[1 + 2\left(\frac{b}{h}\right)\left(\frac{y}{b}\right)\tan\alpha\right]}} \right.$$
$$\left. \cdot \left\{ \xi I_1\left[\frac{h}{b}\sqrt{\frac{1 + 2\left(\frac{b}{h}\right)\left(\frac{y}{b}\right)\tan\alpha}{V\cos\alpha\tan^2\alpha}}\right] - \eta K_1\left[\frac{h}{b}\sqrt{\frac{1 + 2\left(\frac{b}{h}\right)\left(\frac{y}{b}\right)\tan\alpha}{V\cos\alpha\tan^2\alpha}}\right] \right\} \right\rangle \tag{43}$$

The value of $\underline{y/b}$ to be used in equation (43) is that which satisfies

$$2\xi I_1\left[\frac{h}{b}\sqrt{\frac{1 + 2\left(\frac{b}{h}\right)\left(\frac{y}{b}\right)\tan\alpha}{V\cos\alpha\tan^2\alpha}}\right] - 2\eta K_1\left[\frac{h}{b}\sqrt{\frac{1 + 2\left(\frac{b}{h}\right)\left(\frac{y}{b}\right)\tan\alpha}{V\cos\alpha\tan^2\alpha}}\right]$$
$$= \frac{h}{b}\sqrt{\frac{1 + 2\left(\frac{b}{h}\right)\left(\frac{y}{b}\right)\tan\alpha}{V\cos\alpha\tan^2\alpha}} \left\langle \xi \left\{ I_0\left[\frac{h}{b}\sqrt{\frac{1 + 2\left(\frac{b}{h}\right)\left(\frac{y}{b}\right)\tan\alpha}{V\cos\alpha\tan^2\alpha}}\right] \right.\right.$$
$$\left. + I_2\left[\frac{h}{b}\sqrt{\frac{1 + 2\left(\frac{b}{h}\right)\left(\frac{y}{b}\right)\tan\alpha}{V\cos\alpha\tan^2\alpha}}\right] \right\} + \eta \left\{ K_0\left[\frac{h}{b}\sqrt{\frac{1 + 2\left(\frac{b}{h}\right)\left(\frac{y}{b}\right)\tan\alpha}{V\cos\alpha\tan^2\alpha}}\right] \right.$$
$$\left.\left. + K_2\left[\frac{h}{b}\sqrt{\frac{1 + 2\left(\frac{b}{h}\right)\left(\frac{y}{b}\right)\tan\alpha}{V\cos\alpha\tan^2\alpha}}\right] \right\} \right\rangle \tag{44}$$

The coefficients $k_i^{(RECT)}$ give normalized values of sandwich torsional stiffness and maximum facing and core shear stresses in terms of a shear parameter V involving sandwich properties and dimensions.

The coefficients $k_i^{(TRAP)}$ give corresponding normalized values of sandwich torsional stiffness and maximum facing and core shear stresses in terms of the shear parameter V, the angle α defining the slope of the facings relative to the core midplane, and an aspect ratio h/b defining the sandwich thickness to width characteristics, It is noteworthy to observe that these normalized quantities were defined in exactly the same way as their counterparts for the rectangular section, $k_i^{(RECT)}$. As will be seen, this will afford a means of providing direct comparison between calculations for the two cases,

It is apparent from comparison of the expressions given by equations (28), (35), and (41) with those of equations (30), (38), and (43) that presentation of data for trapezoidal sections must of necessity be extremely more complicated than for rectangular sections. In particular, whereas the $k_i^{(RECT)}$ are functions of only the shear parameter V, the $k_i^{(TRAP)}$ are functions of V, α, and h/b. It is possible, however, to facilitate calculations for trapezoidal sections by condensing the expressions for the $k_i^{(TRAP)}$ through the use of a single approximation and the definition of a new variable R defined by

$$R = \frac{\tan\alpha}{h/b} \tag{45}$$

The approximation involves letting $\cos\alpha \to 1$ (i,e., considering only small values of a). Actually, this is not very restrictive--when $\alpha = 20°$ (a highly trapezoidal section), $\cos\alpha \approx 0.94$. The motivation for making this reasonable approximation is simply to provide a means of obtaining expressions for the $k_i^{(TRAP)}$ which are functions of only two variables--V and R. Making these substitutions within the expressions for these normalized quantities yields

$$\frac{1}{k_1^{(TRAP)}} \approx 1 + 2R + \frac{4}{3}R^2 + 4VR^2 + 4VR^3 + 8V^2R^3\left\{\xi\left[\frac{\phi}{2}\left(\frac{\phi^2}{4}+1\right)I_1(\phi) - \frac{\psi}{2}\left(\frac{\psi^2}{4}+1\right)I_1(\psi) - \frac{\phi^2}{4}I_0(\phi) + \frac{\psi^2}{4}I_0(\psi)\right] - \eta\left[\frac{\phi}{2}\left(\frac{\phi^2}{4}+1\right)K_1(\phi) - \frac{\psi}{2}\left(\frac{\psi^2}{4}+1\right)K_1(\psi) + \frac{\phi^2}{4}K_0(\phi) - \frac{\psi^2}{4}K_0(\psi)\right]\right\} \tag{46}$$

where

$$\xi \approx \frac{(1 + 4VR^2)K_0(\phi) - (1 + 2R + 4VR^2)K_0(\psi)}{I_0(\phi)K_0(\psi) - I_0(\psi)K_0(\phi)}$$

$$\eta \approx \frac{(1 + 2R + 4VR^2)I_0(\psi) - (1 + 4VR^2)I_0(\phi)}{I_0(\phi)K_0(\psi) - I_0(\psi)K_0(\phi)} \tag{47}$$

and

$$\psi \approx \frac{1}{R\sqrt{V}}$$

$$\phi \approx \frac{\sqrt{1 + 2R}}{R\sqrt{V}} \tag{48}$$

Furthermore,

$$k_2^{(TRAP)} \approx k_1^{(TRAP)} \left\{ 1 + 2R\left(\frac{y}{b}\right) + 4VR^2 + \xi I_0\left[\frac{1}{R}\sqrt{\frac{1 + 2R\left(\frac{y}{b}\right)}{V}}\right] + \eta K_0\left[\frac{1}{R}\sqrt{\frac{1 + 2R\left(\frac{y}{b}\right)}{V}}\right] \right\} \tag{49}$$

where <u>y/b</u> is the solution of

$$\eta K_1\left[\frac{1}{R}\sqrt{\frac{1 + 2R\left(\frac{y}{b}\right)}{V}}\right] - \xi I_1\left[\frac{1}{R}\sqrt{\frac{1 + 2R\left(\frac{y}{b}\right)}{V}}\right] = 2R\sqrt{V\left[1 + 2R\left(\frac{y}{b}\right)\right]} \tag{50}$$

Finally,

$$k_3^{(TRAP)} \approx k_1^{(TRAP)}\sqrt{V}\,R \left\langle 2 + \frac{1/R}{\sqrt{V\left[1 + 2R\left(\frac{y}{b}\right)\right]}} \left\{ \xi I_1\left[\frac{1}{R}\sqrt{\frac{1 + 2R\left(\frac{y}{b}\right)}{V}}\right] - \eta K_1\left[\frac{1}{R}\sqrt{\frac{1 + 2R\left(\frac{y}{b}\right)}{V}}\right] \right\} \right\rangle \tag{51}$$

where y/b is the solution of

$$2\xi I_1\left[\frac{1}{R}\sqrt{\frac{1+2R\left(\frac{y}{b}\right)}{V}}\right] - 2\eta K_1\left[\frac{1}{R}\sqrt{\frac{1+2R\left(\frac{y}{b}\right)}{V}}\right]$$

$$= \frac{1}{R}\sqrt{\frac{1+2R\left(\frac{y}{b}\right)}{V}} \left\langle \xi\left\{ I_0\left[\frac{1}{R}\sqrt{\frac{1+2R\left(\frac{y}{b}\right)}{V}}\right] + I_2\left[\frac{1}{R}\sqrt{\frac{1+2R\left(\frac{y}{b}\right)}{V}}\right]\right\}\right. \tag{52}$$

$$\left. + \eta\left\{ K_0\left[\frac{1}{R}\sqrt{\frac{1+2R\left(\frac{y}{b}\right)}{V}}\right] + K_2\left[\frac{1}{R}\sqrt{\frac{1+2R\left(\frac{y}{b}\right)}{V}}\right]\right\}\right\rangle$$

The coefficients $k_i^{(TRAP)}$ have now been presented in terms of two independent variables--a shear parameter V defined exactly as in the case of the rectangular section, and a shape parameter R defining the deviation of the trapezoidal section from a rectangular section. It is obvious that as the parameter R approaches zero (i.e., $\alpha \to 0$) the trapezoidal section converges to a rectangular section. Accordingly, taking the limit as R approaches zero of the $k_i^{(TRAP)}$ should yield the $k_i^{(RECT)}$. Inspection, however, of equations (46), (49), and (51) reveals the impracticability of accomplishing this limiting process analytically to reduce these equations to the forms of equations (28), (35), and (41), respectively. Subsequent numerical calculations for the $k_i^{(TRAP)}$ did converge to calculations for the $k_i^{(RECT)}$ for decreasing values of R.

Triangular sections.--Introduce the shear parameter W defined by

$$W = \frac{tG}{2bG_c} \tag{53}$$

Upon making this substitution, it becomes possible to write equation (25) into the form

$$\frac{T}{\theta/L} = \frac{8tb^3G}{k_1^{(TRI)}} \tag{54}$$

where

$$\frac{1}{k_1^{(TRI)}} = \sin\alpha\tan\alpha \left\langle \frac{1}{3} + W\sin\alpha - \frac{1+2W\sin\alpha}{I_0\left(\sqrt{\frac{2}{W\sin\alpha}}\right)}\left\{\sqrt{2W\sin\alpha}\, I_1\left(\sqrt{\frac{2}{W\sin\alpha}}\right)\right.\right.$$

$$\left.\left. - (2W\sin\alpha) I_2\left(\sqrt{\frac{2}{W\sin\alpha}}\right)\right\}\right\rangle \tag{55}$$

Proceeding in the same manner as with the rectangular and trapezoidal sections, the maximum facing shear stress becomes expressible in the form

$$\tau_{MAX} = \frac{T}{4tb^2} k_2^{(TRI)} \tag{56}$$

where

$$k_2^{(TRI)} = k_1^{(TRI)} \sin\alpha \left\{ \frac{y}{b} + 2W\sin\alpha - (1 + 2W\sin\alpha) \frac{I_0\left(\sqrt{\frac{2\left(\frac{y}{b}\right)}{W\sin\alpha}}\right)}{I_0\left(\sqrt{\frac{2}{W\sin\alpha}}\right)} \right\} \tag{57}$$

and y/b is the solution of

$$(1 + 2W\sin\alpha)\, I_1\left(\sqrt{\frac{2\left(\frac{y}{b}\right)}{W\sin\alpha}}\right) = \sqrt{2\left(\frac{y}{b}\right)W\sin\alpha}\; I_0\left(\sqrt{\frac{2}{W\sin\alpha}}\right) \tag{58}$$

The maximum core shear stress can be written as

$$\tau_{c_{MAX}} = \frac{T}{4b^3} k_3^{(TRI)}$$

where

$$k_3^{(TRI)} = k_1^{(TRI)} \sin\alpha \left\{ 1 - \frac{1 + 2W\sin\alpha}{\sqrt{2\left(\frac{y}{b}\right)W\sin\alpha}} \frac{I_1\left(\sqrt{\frac{2\left(\frac{y}{b}\right)}{W\sin\alpha}}\right)}{I_0\left(\sqrt{\frac{2}{W\sin\alpha}}\right)} \right\} \tag{59}$$

and y/b is the solution of

$$I_2\left(\sqrt{\frac{2\left(\frac{y}{b}\right)}{W\sin\alpha}}\right) = C \tag{60}$$

There being no real solution to equation (60), the core shear stress value sought is a relative maximum (or minimum, since absolute value is desired) on the

interval $0 \leq y \leq b$. It will be pointed out that this same conclusion was reached numerically for the trapezoidal section and that, for both the triangular and trapezoidal section, the maximum core shear stress always occurred at the thick edge defined by $y = b$.

The coefficients $k_i^{(TRI)}$ give normalized values of sandwich torsional stiffness and maximum facing and core shear stresses in terms of a shear parameter W involving sandwich properties and dimensions, and an angle α defining the "triangularity" of the section.

5. Numerical Calculations and Design Curves

To facilitate utilization of the analytical expressions derived for torsional stiffness, maximum facing shear stress, and maximum core shear stress, the normalized quantities $k_i^{(RECT)}$, $k_i^{(TRAP)}$, and $k_i^{(TRI)}$ are presented in a series of design curves. In all cases, these design coefficients are plotted versus the appropriate shear parameter (V or W) and, if required, presented in families of curves (in R or α).

A summary of the manner in which the design parameters are defined for each section, as well as the pertinent equations for their calculations, is provided in table 1.

The design coefficients $k_i^{(RECT)}$, as given by equations (28), (35), and (41), are presented in figures 4 and 5 versus the shear parameter V. One especially interesting result arises from equation (34) when the core is rigid, for which $G_c \to \infty$ and, consequently, $V \to 0$. In particular,

$$\tau_{MAX} \to \frac{T}{2thb} \tag{61}$$

Equation (61) is in agreement with the well-known results predicted by the elastic membrane ("soap-film") analogy for torsion of thin-walled sections (Trayer and March). [5]

The data presented in figures 4 and 5, and in all subsequent figures, were obtained through the use of the U.S. Forest Products Laboratory math and computer facilities with its IBM 1620 system, and the facilities of the University of Wisconsin Computing Center with its Univac 1108 system.

Presentation of design data for torsion of trapezoidal and triangular sections cannot be presented in as concise a form as for rectangular sections. The forms of the $k_i^{(TRAP)}$ and $k_i^{(TRI)}$ necessitate presentation of these quantities in families of curves.

---

[5] Trayer, G. W., and March, H. W. The Torsion of Members Having Sections Common in Aircraft Construction. Nat. Adv. Comm. Aeron. Rep. 334. 1930.

Figures 6 through 15 present the design coefficients $k_i^{(TRAP)}$ plotted, in families of curves in $R = \frac{\tan\alpha}{h/b}$, versus the shear parameter V. Superimposed on appropriate figures are the plots of figure 4 for the $k_i^{(RECT)}$, to illustrate the correct convergence of the trapezoidal section results.

Figures 16 through 21 present the design coefficients $k_i^{(TRI)}$ plotted, in families of curves in α, versus the shear parameter W. Values of all coefficients were calculated for values of V or W as small as was practicable within the framework of the computer routines[6] used to calculate the required modified Bessel functions,

Calculations for the normalized maximum facing and core shear stresses (k_2 and k_3, respectively) involved essentially two parts, the first of which involved obtaining the solution of an appropriate transcendental equation for the location of the maximum value. The roots to these equations were obtained numerically via an iterative scheme. It is noteworthy to point out that for both the trapezoidal and the triangular sections, the maximum core shear stress in all cases occurred as a relative maximum in the interval $0 \leq \frac{y}{b} \leq 1$ at the "thick" edge defined by $y = b$. It is also noteworthy to mention that the location of the maximum facing shear stress in the trapezoidal section approached the value $y = \frac{b}{2}$ for small values of α, in agreement with closed-form results for the rectangular section,

Summary

The theory and solutions of Cheng have been extended to provide design data for torsion of sandwich strips of triangular, rectangular, and trapezoidal cross sections. Detailed derivations for torsional stiffness, maximum facing shear stress, and maximum core shear stress have been presented. Normalized values of these quantities have been expressed as design coefficients and set forth in a series of design curves versus appropriate shear parameters. Data for trapezoidal and triangular sections have, of necessity, been presented in families of curves in geometric parameters expressing the variation of these sections from rectangular sections.

Data obtained for trapezoidal sections have been approximated to facilitate presentation of results, and the degree of approximation decreases as these sections become less "trapezoidal."

Direct comparison of data is shown on the curves for design coefficients of trapezoidal sections and rectangular sections, with correct convergence obtained in the proper limits. Values of the design coefficients for cores of infinite shear rigidity have been obtained expressly for rectangular sections, but could only be approximated from the design curves for the other two sections because of mathematical and, hence, computational unmanageability.

All data presented have been obtained from the analytical derivations through the use of appropriate digital computer systems and, when necessary, with the aid of specific programing routines to evaluate complicated mathematical functions.

---

[6] Sperry-Rand Corporation. Math-Pack. Univac Large-Scale Systems . Philadelphia, Pa. 1970.

Table 1.--Definitions of design parameters and summary of equations[1] used in their calculations

Design parameter	Sandwich section		
	Rectangular	Trapezoidal	Triangular
k_1	$\frac{2th^2bG}{\left(\frac{T}{\theta/L}\right)}$ [28]	$\frac{2th^2bG}{\left(\frac{T}{\theta/L}\right)}$ [46]	$\frac{8tb^3G}{\left(\frac{T}{\theta/L}\right)}$ [55]
k_2	$\frac{\tau_{MAX}}{(T/2thb)}$ [35]	$\frac{\tau_{MAX}}{(T/2thb)}$ [49]	$\frac{\tau_{MAX}}{(T/4tb^2)}$ [57]
k_3	$\frac{\tau_{c_{MAX}}}{(T\sqrt{2G_c}/2hb\sqrt{thG})}$ [41]	$\frac{\tau_{c_{MAX}}}{(T\sqrt{2G_c}/2hb\sqrt{thG}}$ [51]	$\frac{\tau_{c_{MAX}}}{(T/4b^3)}$ [59]

[1]The number in brackets below each term indicates the applicable equation from the text.

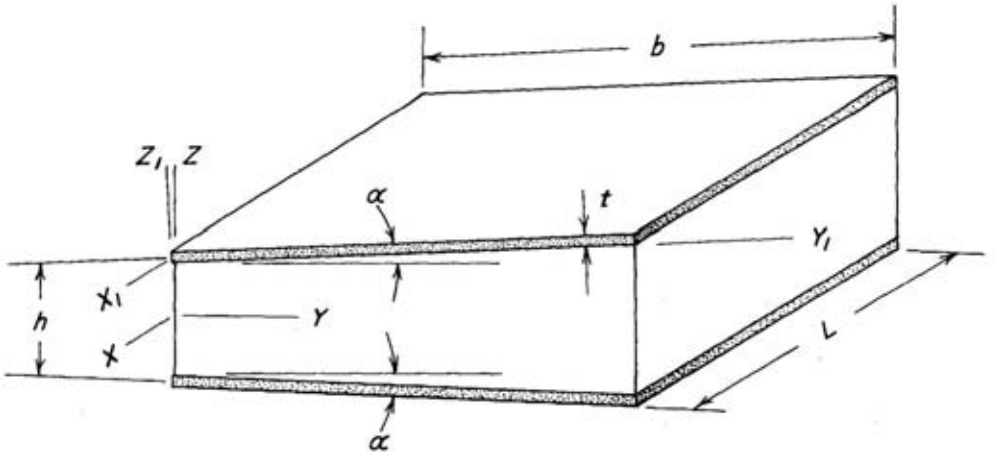

Figure 1.--Sandwich with trapezoidal cross section.

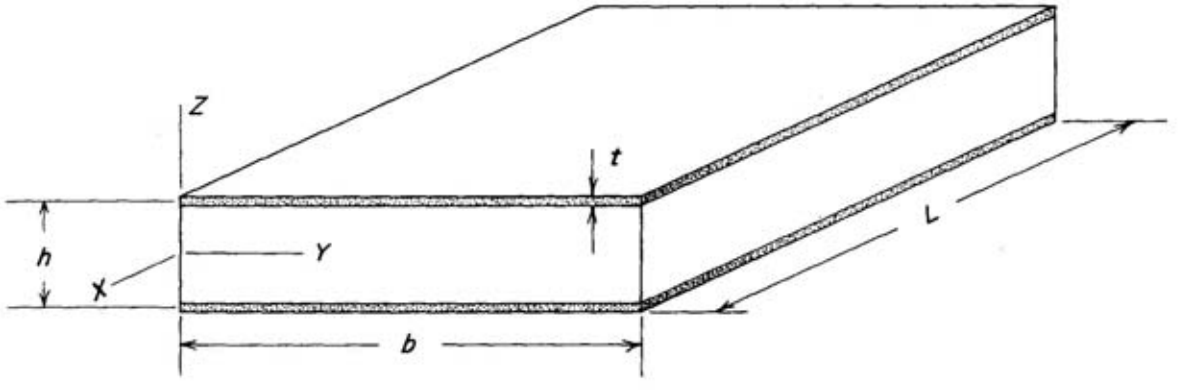

Figure 2.--Sandwich with rectangular cross section.

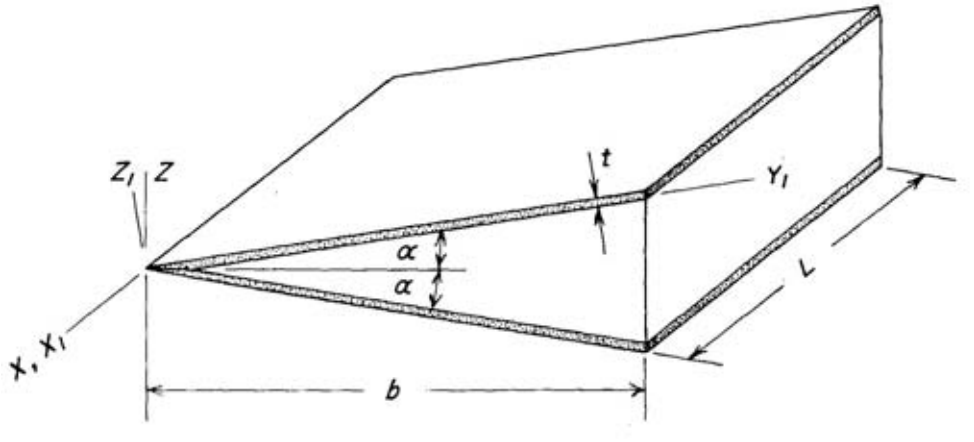

Figure 3.--Sandwich with triangular cross section.

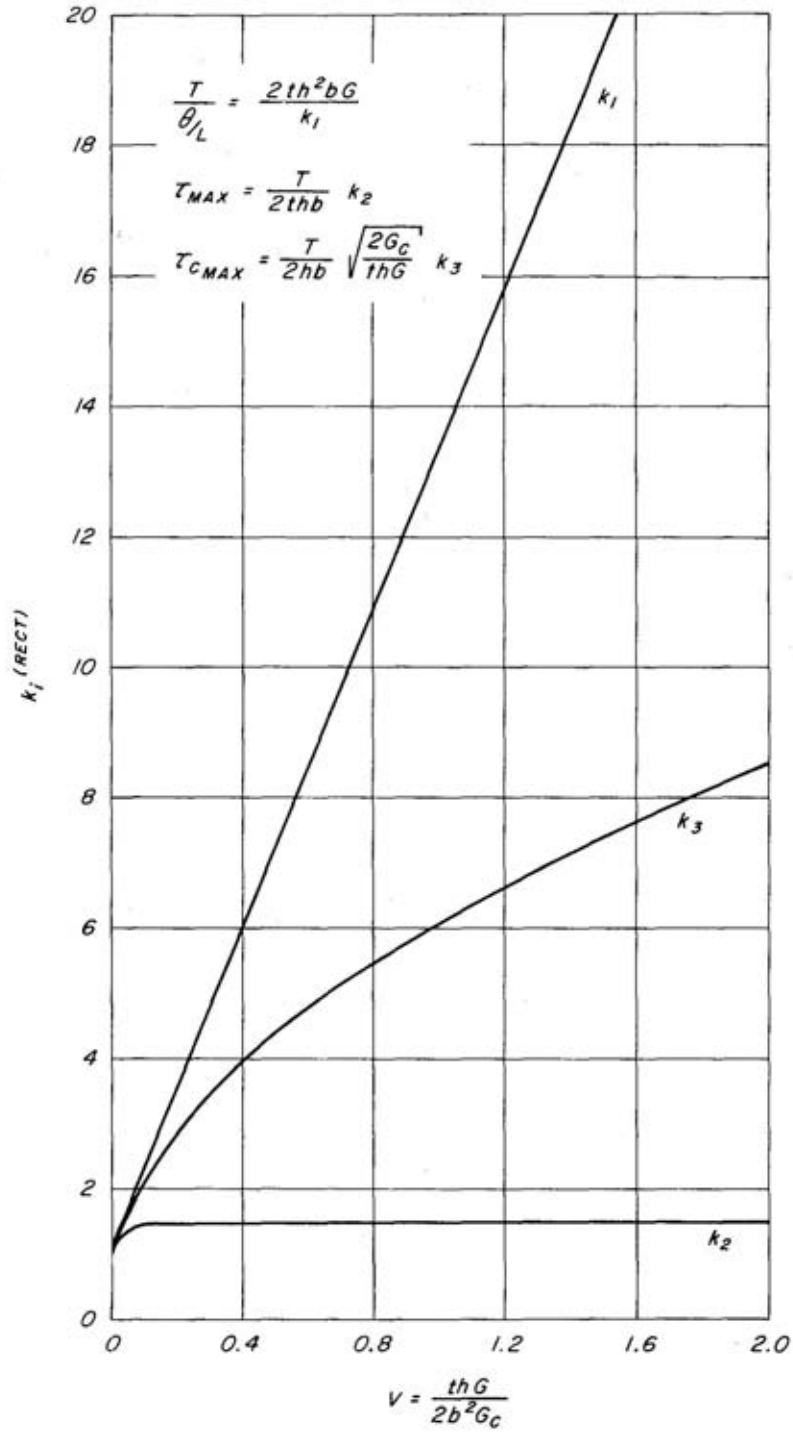

Figure 4.--Design coefficients for rectangular sections. M 140 392

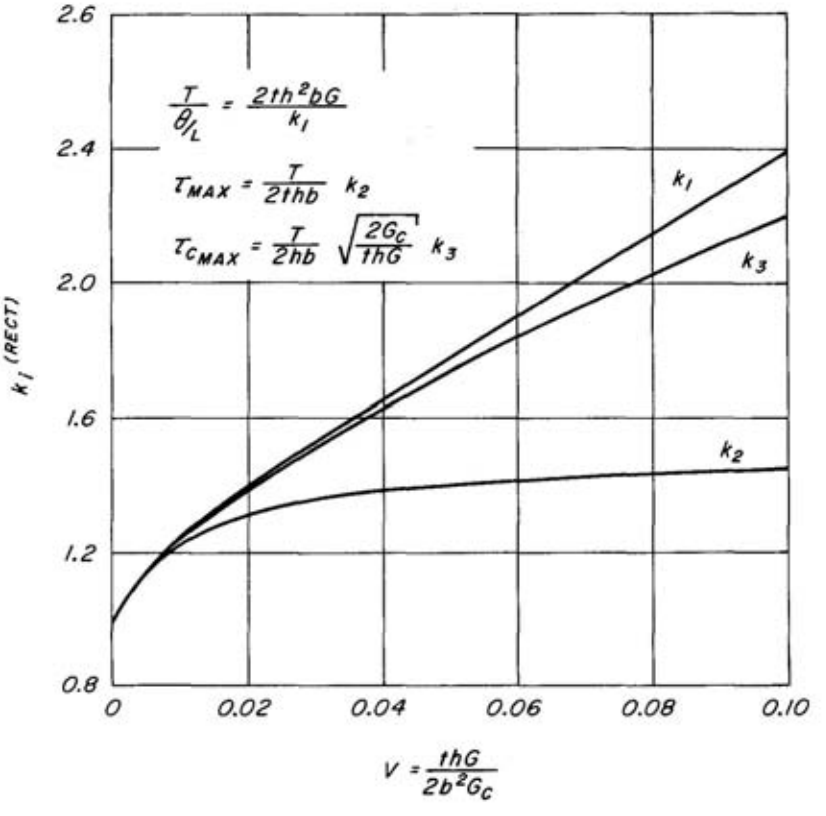

Figure 5.--Design coefficients for rectangular sections--stiff cores,

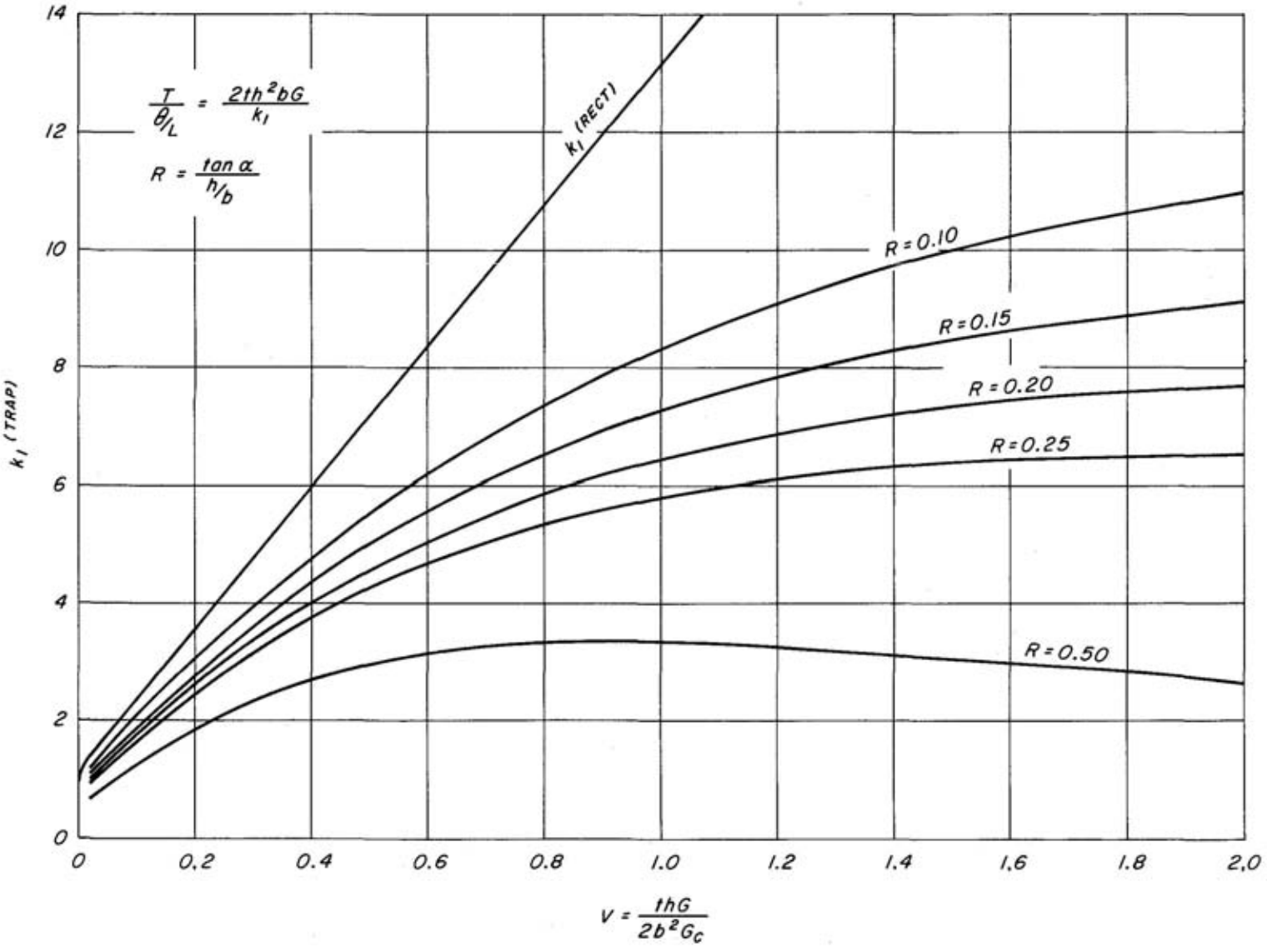

Figure 6.––Normalized torsional stiffness for trapezoidal sections. R = 0.10, 0.15, 0.20, 0.25, 0.50.

M 140 395

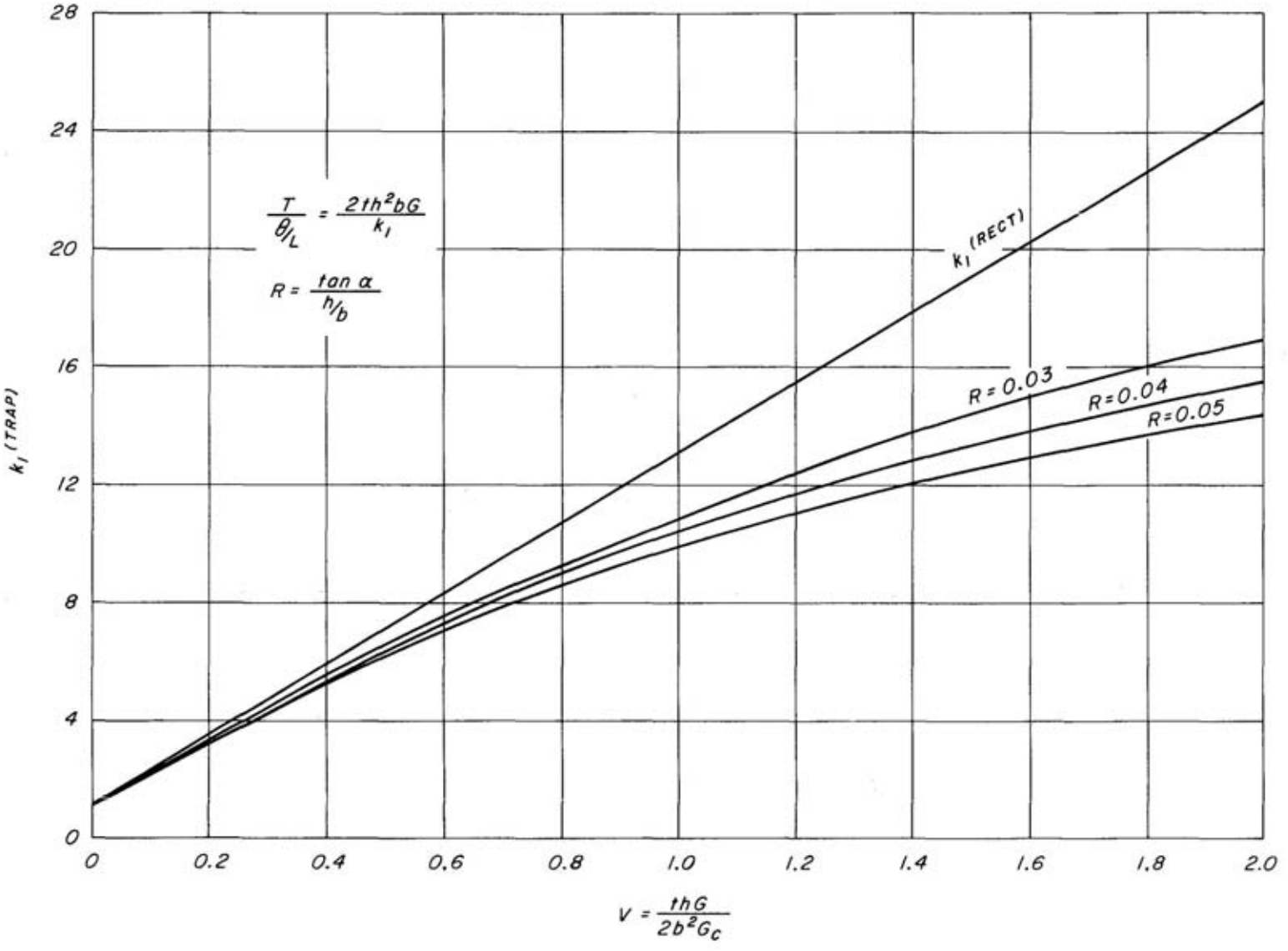

Figure 7.--Normalized torsional stiffness for trapezoidal sections. R = 0.03, 0.04, 0.05. M 140 403

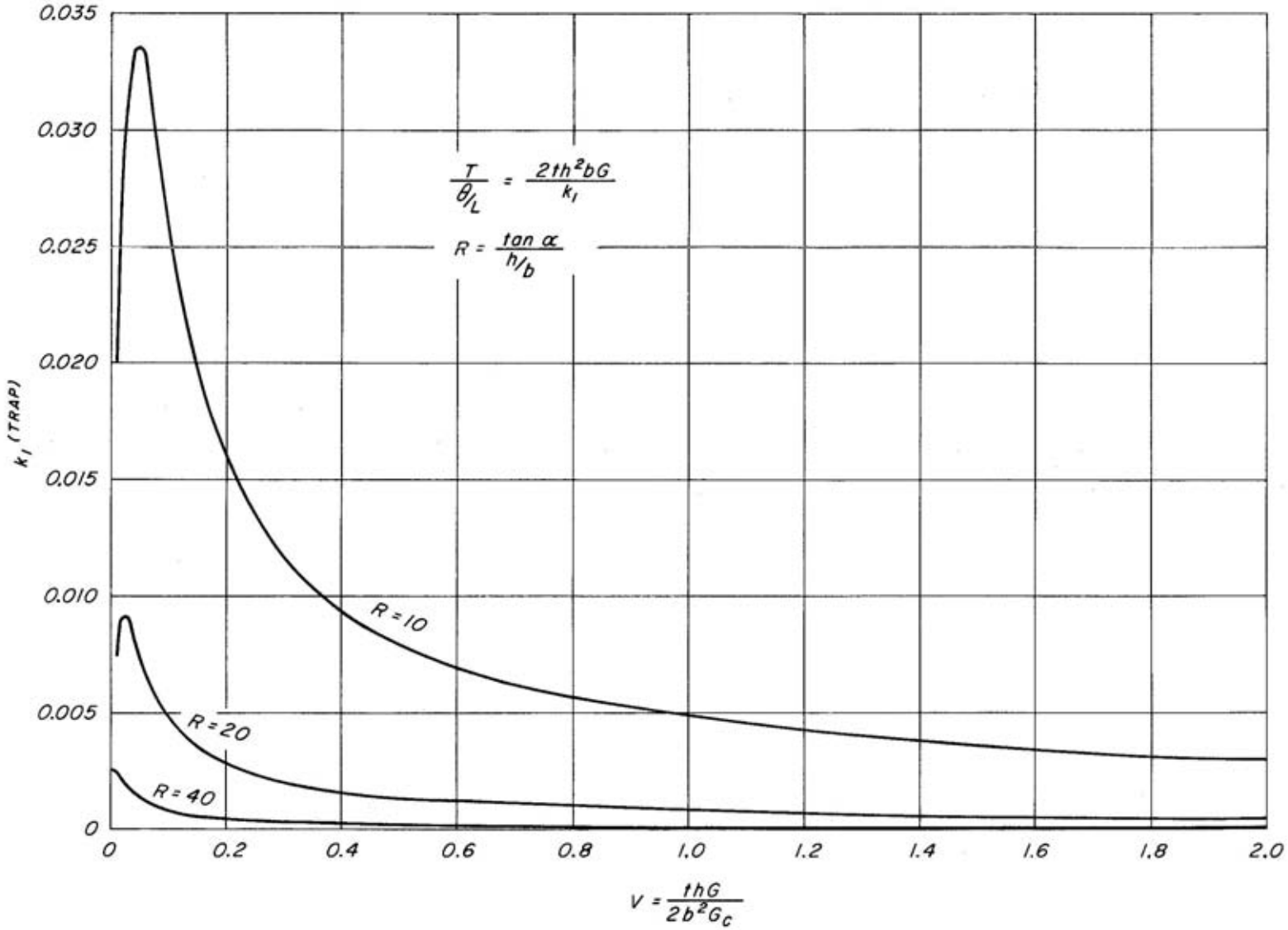

Figure 8.--Normalized torsional stiffness for trapezoidal sections. R = 10, 20, 40.

M 140 399

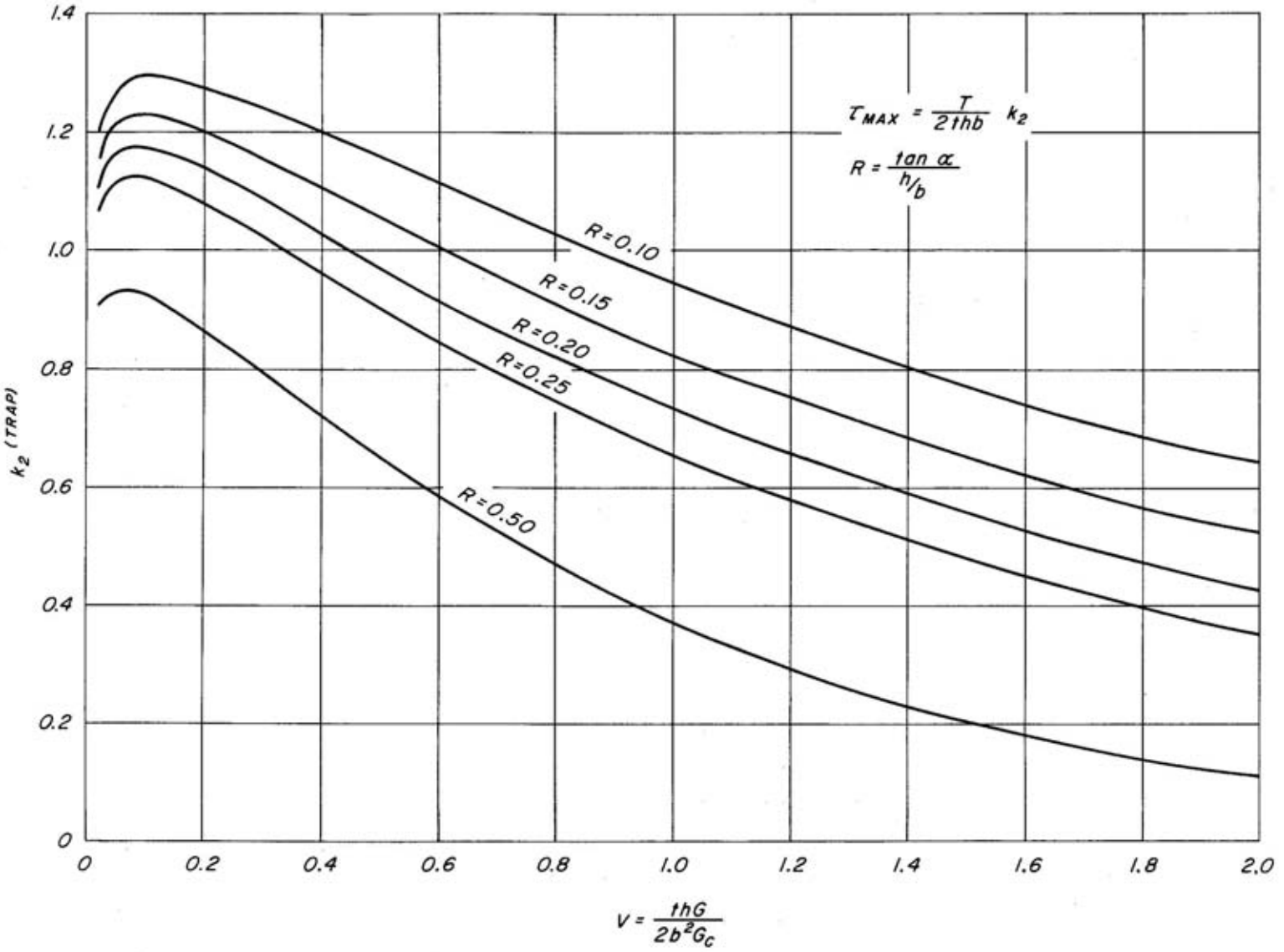

Figure 9.––Normalized maximum facing shear stress for trapezoidal sections, R = 0.10, 0.15, 0.20, 0.25, 0.50. M 140 402

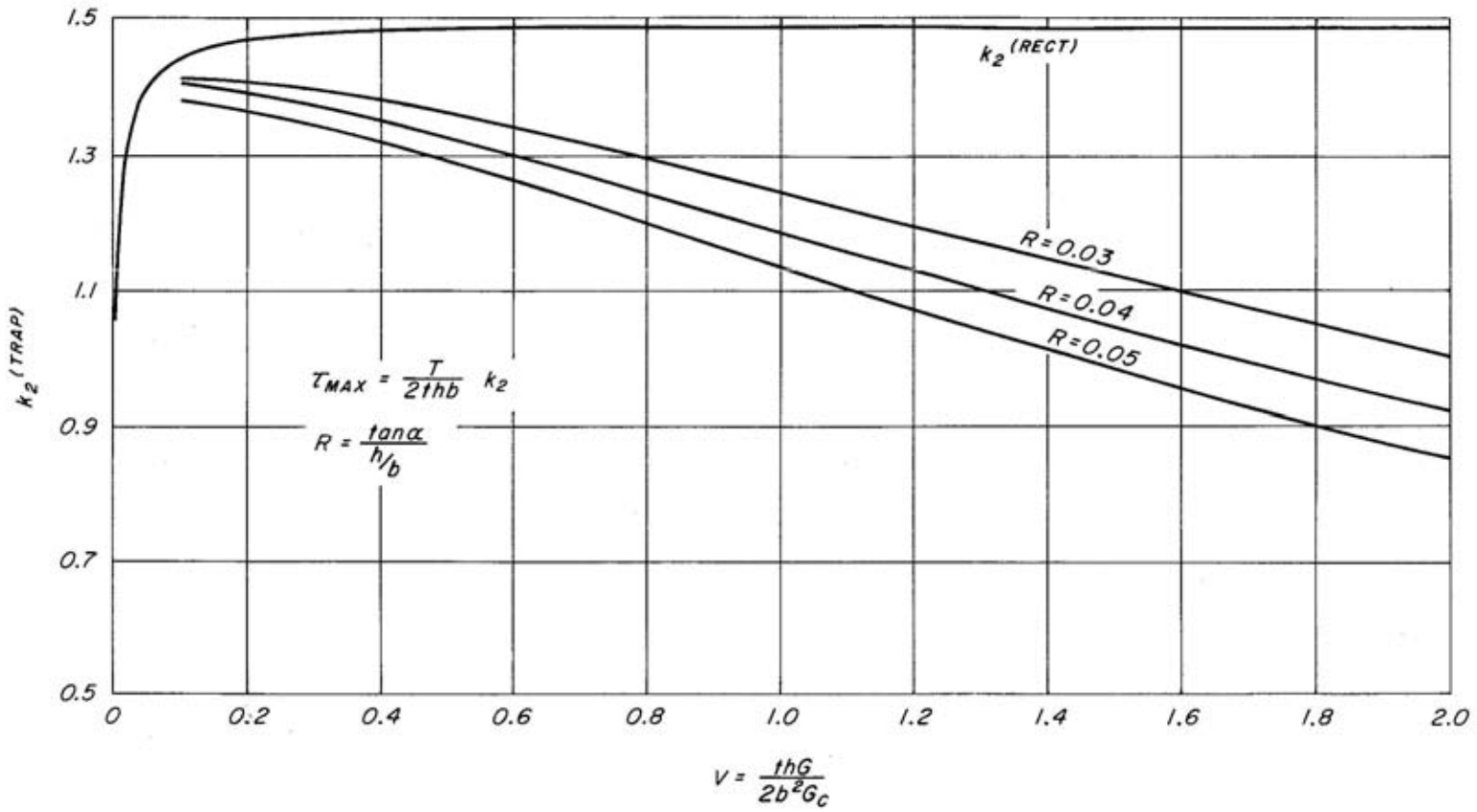

Figure 10.--Normalized maximum facing shear stress for trapezoidal sections. R = 0.03, 0.04, 0.05. M 140 409

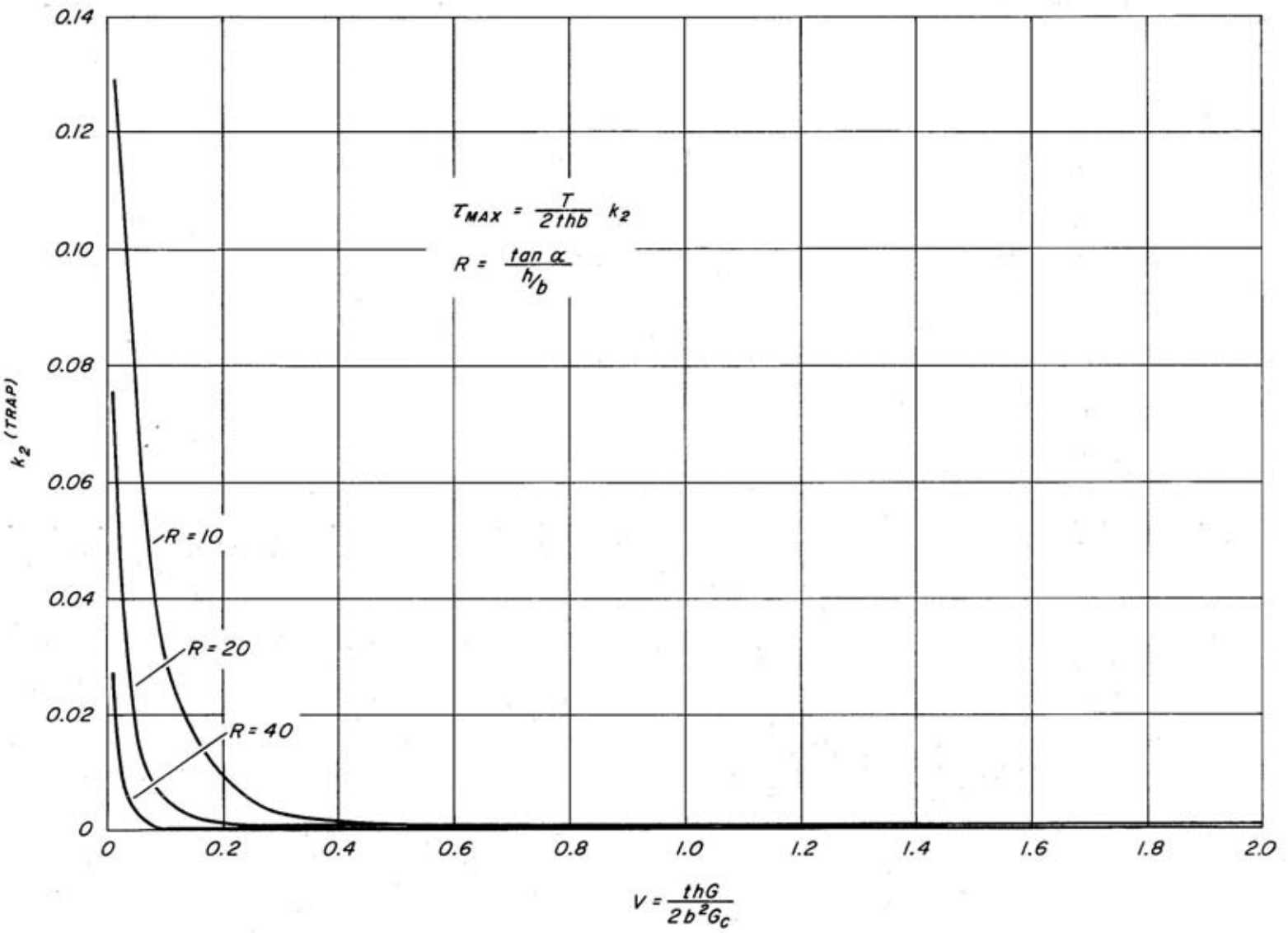

Figure 11.––Normalized maximum facing shear stress for trapezoidal sections. R = 10, 20, 40. M 140 408

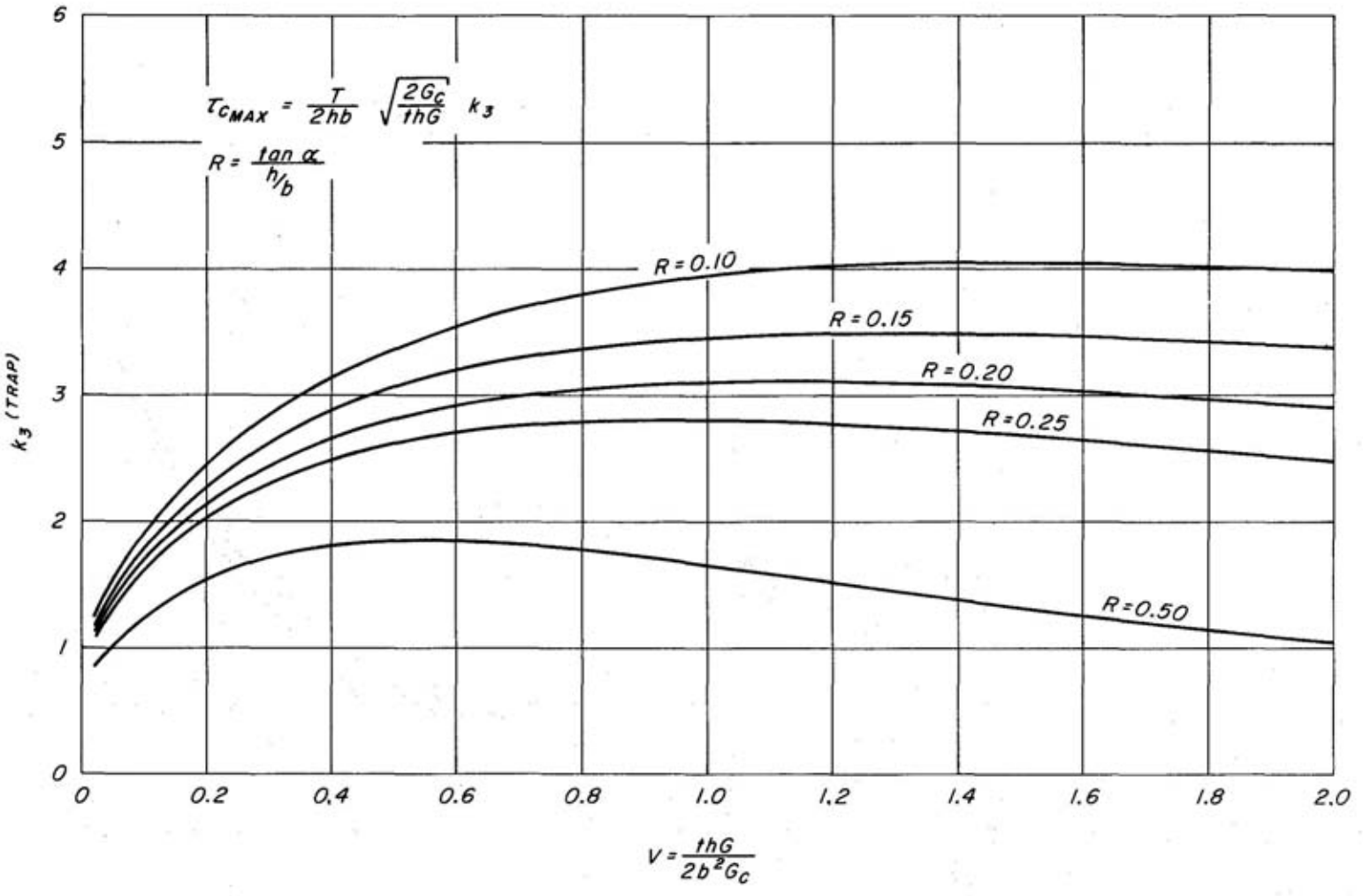

Figure 12.--Normalized maximum core shear stress for trapezoidal sections. R = 0.10, 0.15, 0.20, 0.25, 0.50. M 140 406

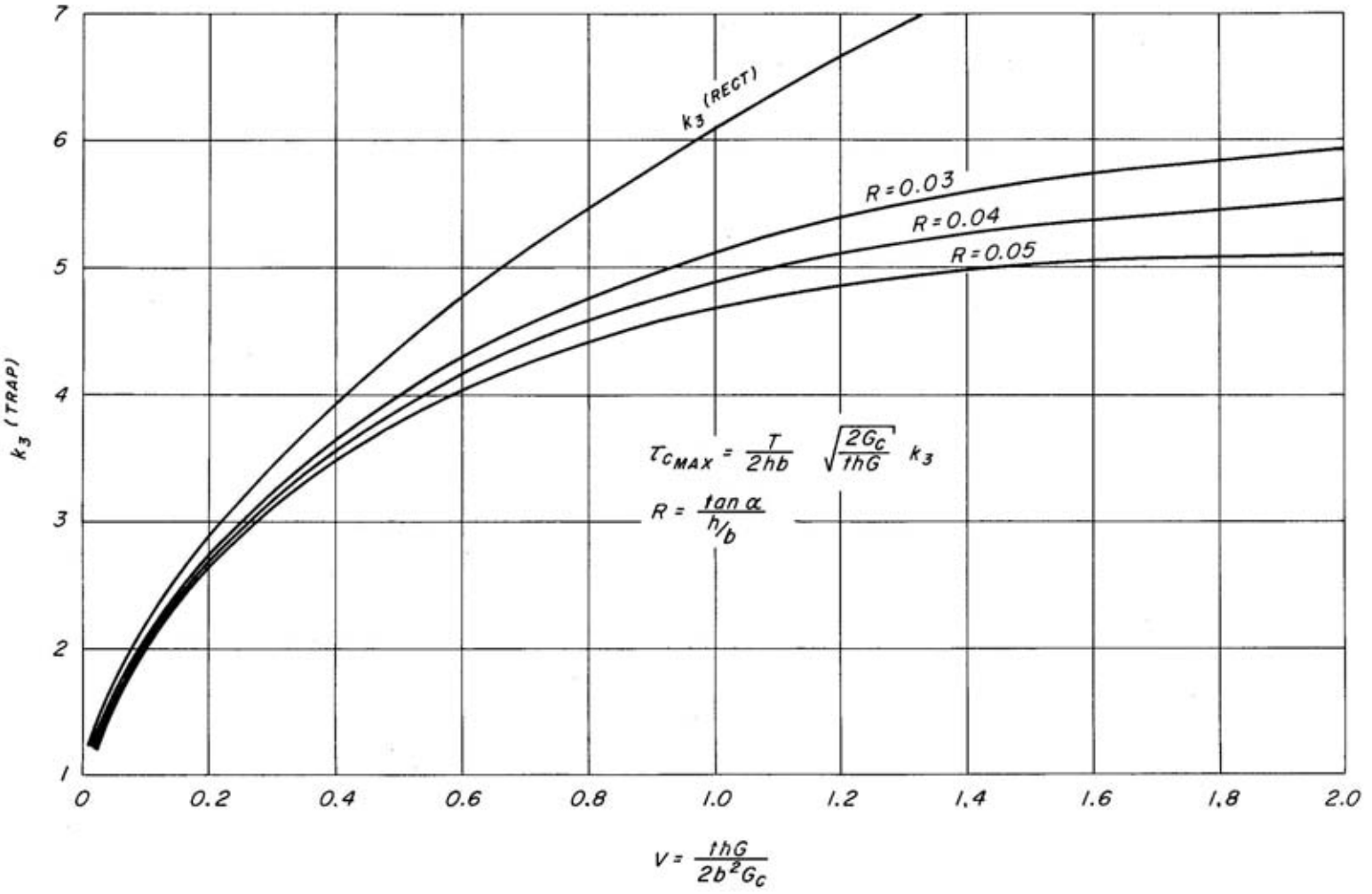

Figure 13.––Normalized maximum core shear stress for trapezoidal sections. R = 0.03, 0.04, 0.05. M 140 404

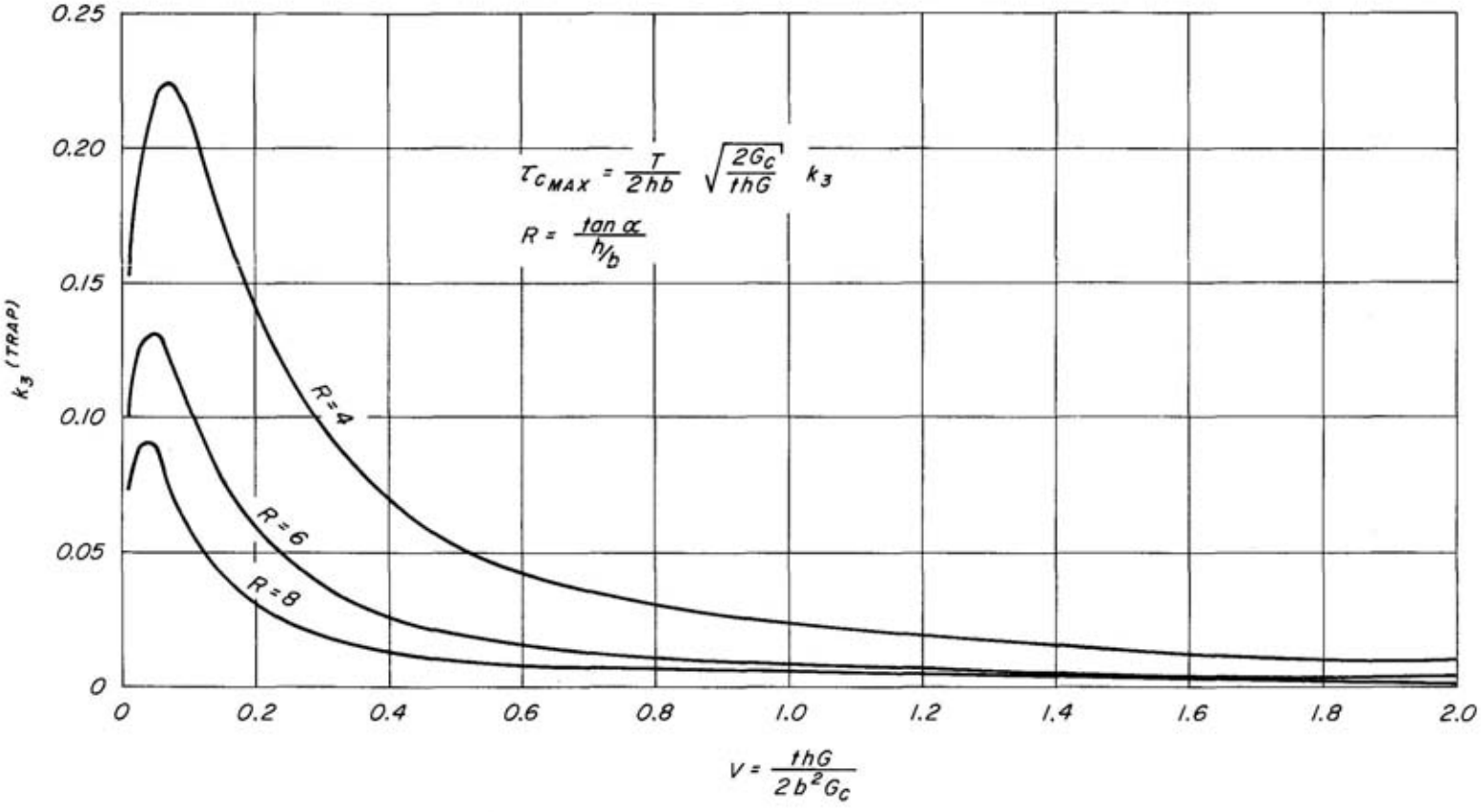

Figure 14.––Normalized maximum core shear stress for trapezoidal sections. R = 4, 6, 8. M 140 397

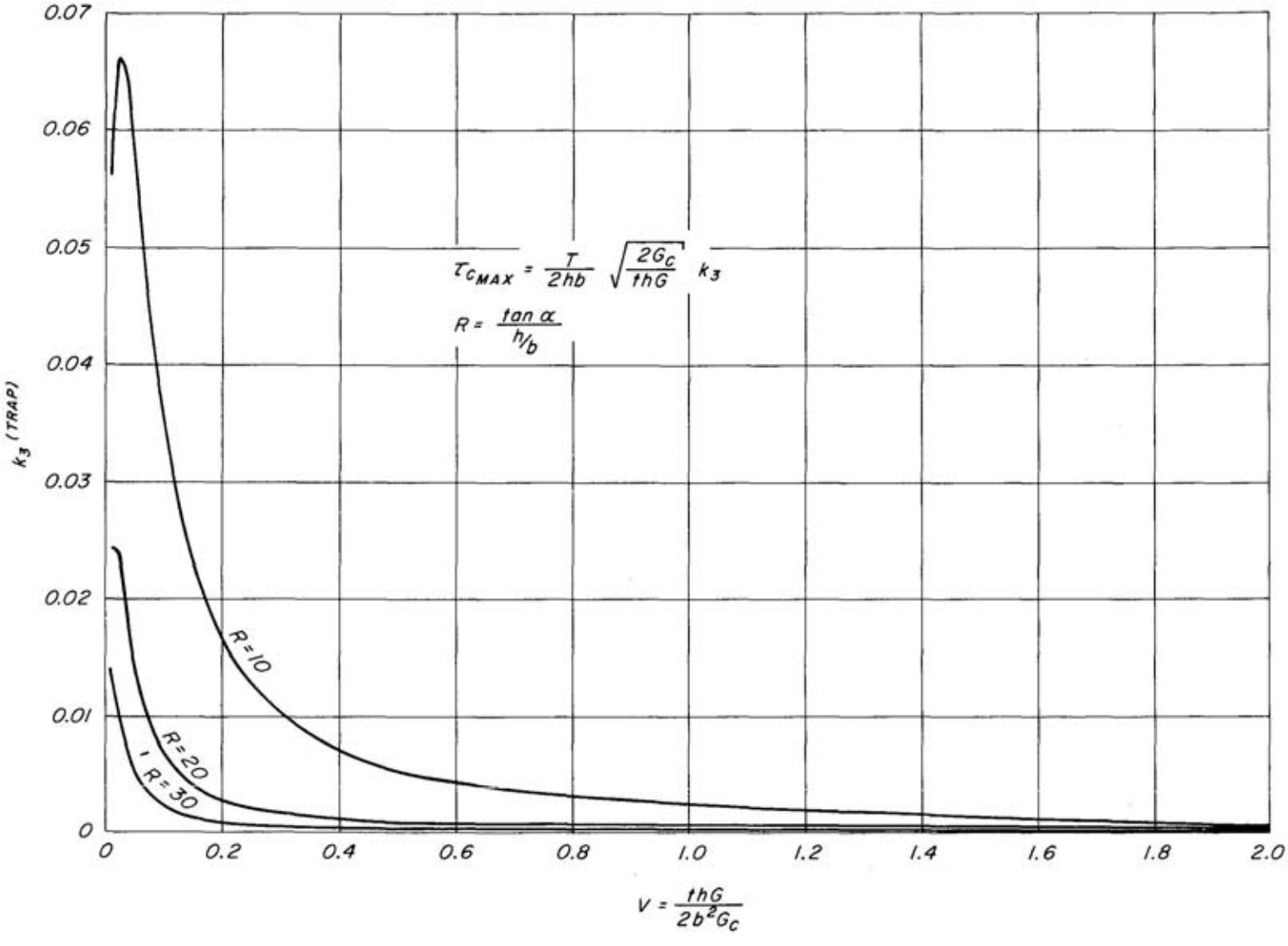

Figure 15.––Normalized maximum core shear stress for trapezoidal sections. R = 10, 20, 30. M 140 398

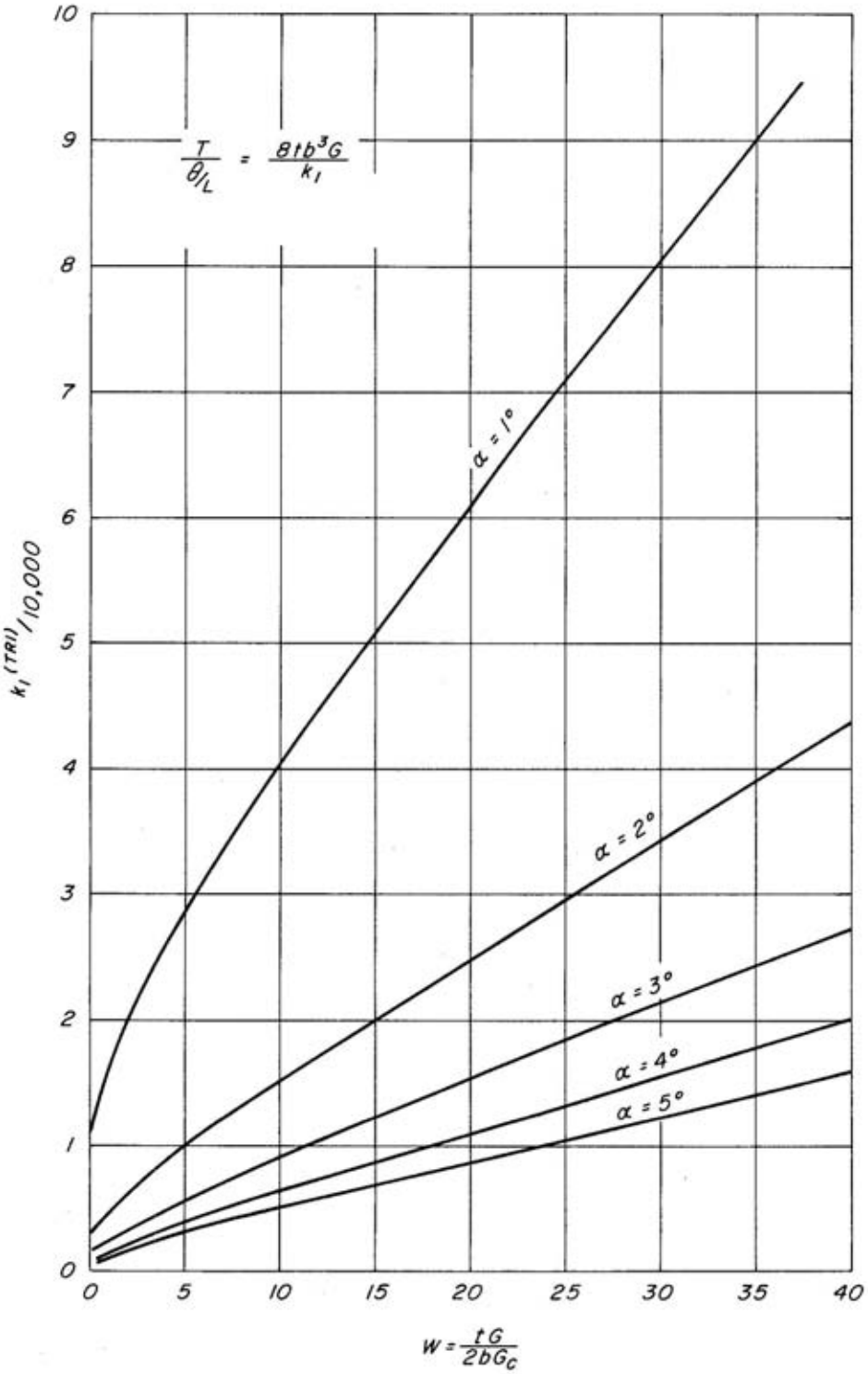

Figure 16.--Normalized torsional stiffness for triangular sections. a = 1°, 2°, 3°, 4°, 5°. M 140 407

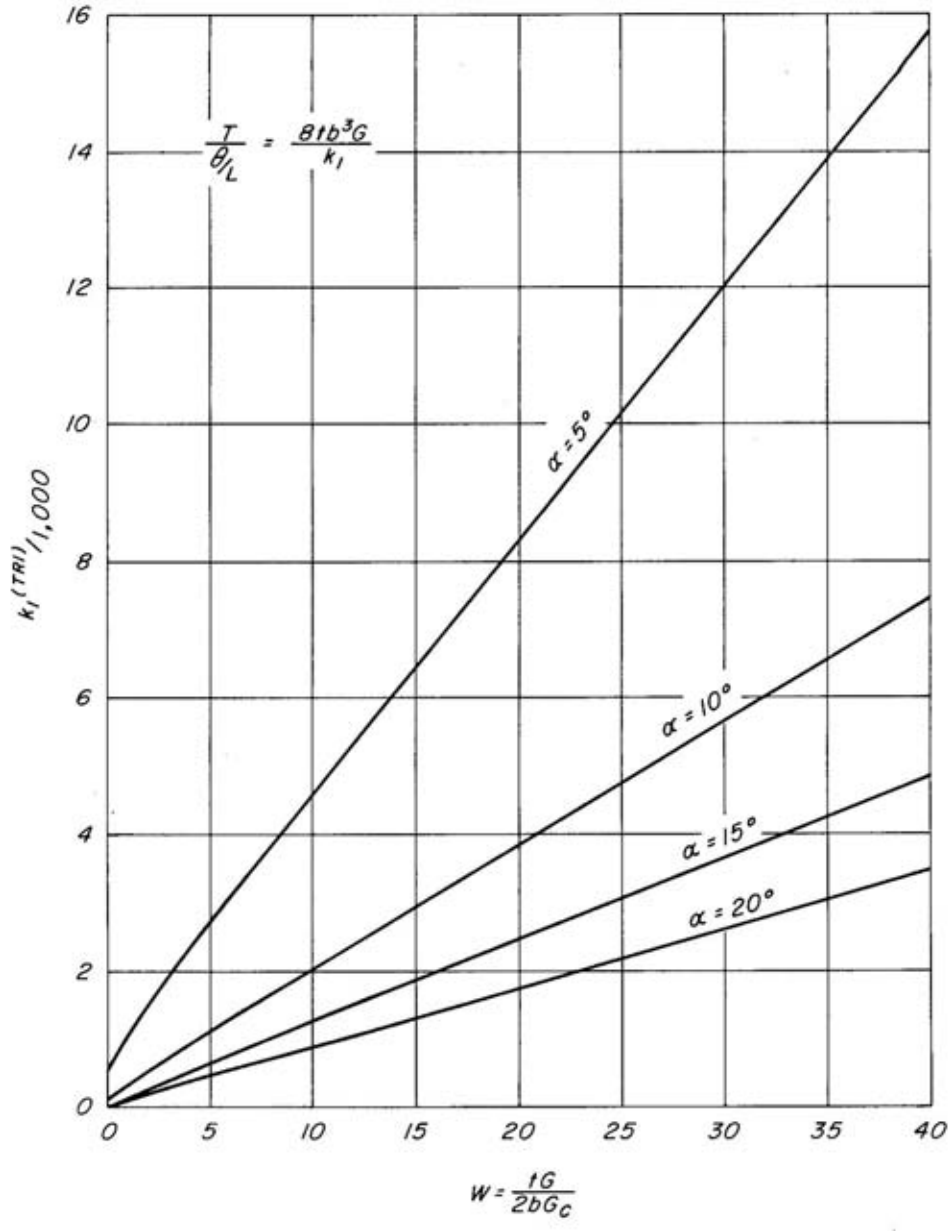

Figure 17.--Normalized torsional stiffness for triangular sections. α = 5°, 10°, 15°, 20°. M 140 401

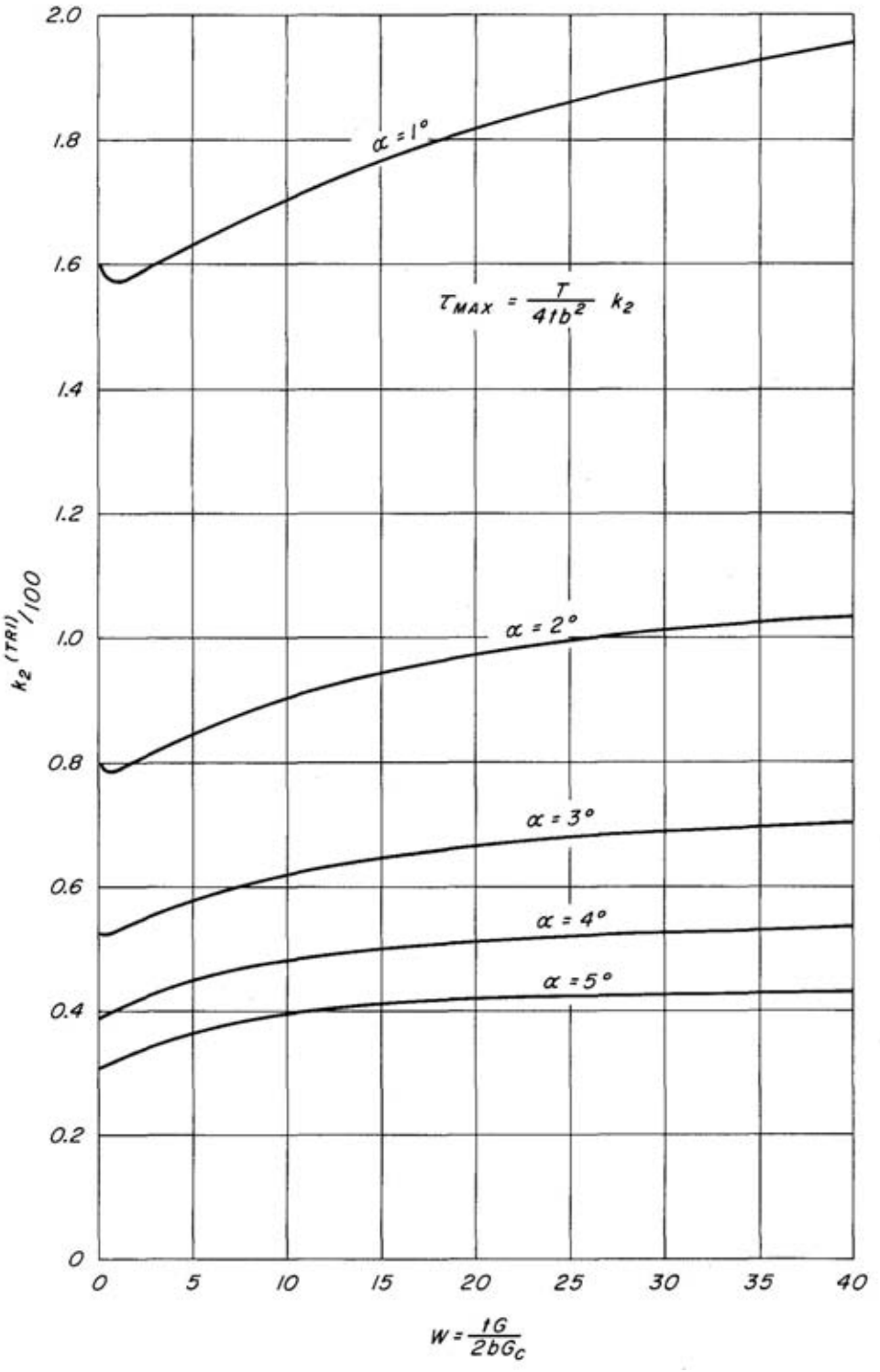

Figure 18.--Normalized maximum facing shear stress for triangular sections. α = 1°, 2°, 3°, 4°, 5°. M 140 410

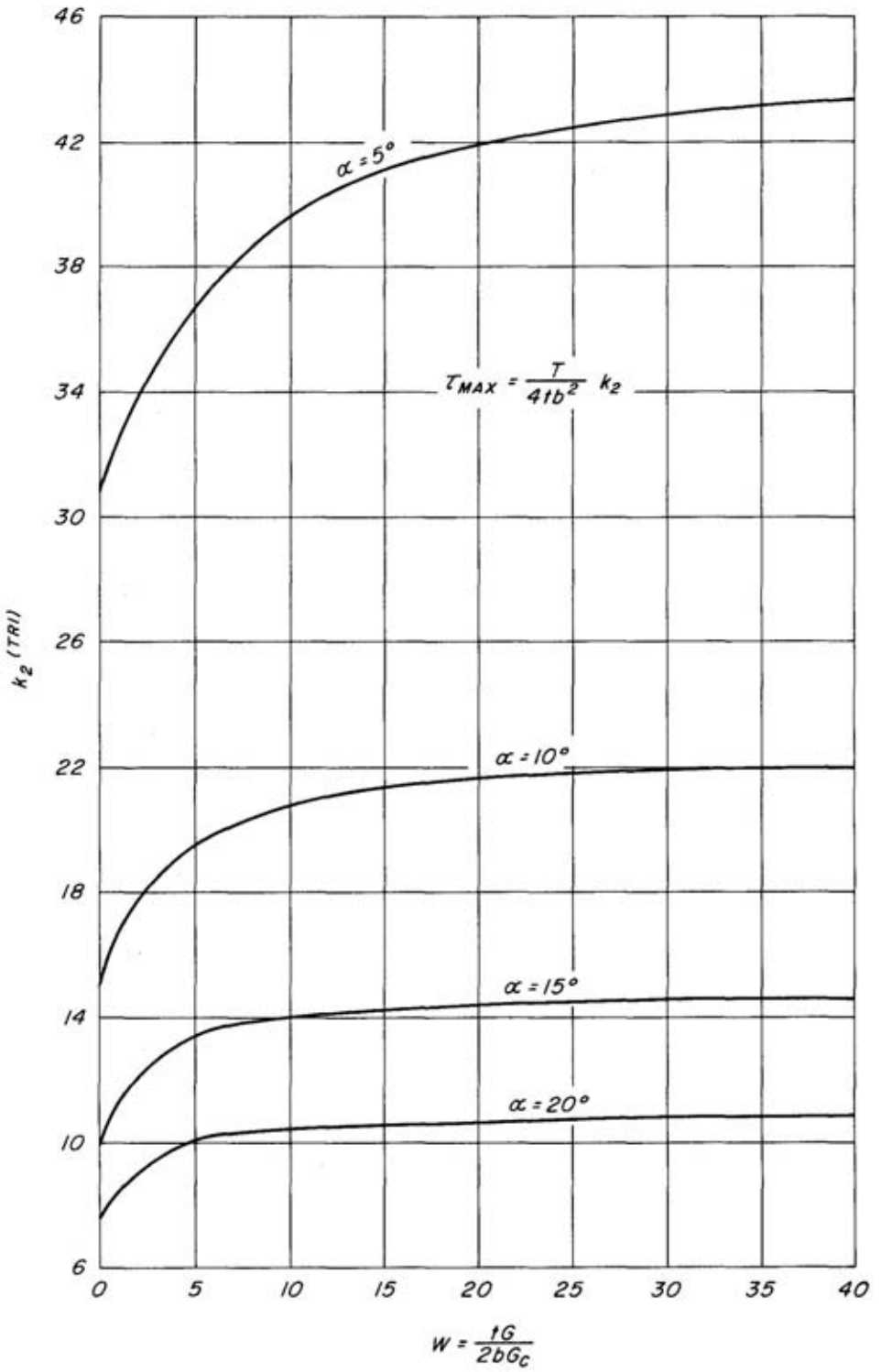

Figure 19.––Normalized maximum facing shear stress for triangular sections. R = 5°, 10°, 15°, 20°. M 140 394

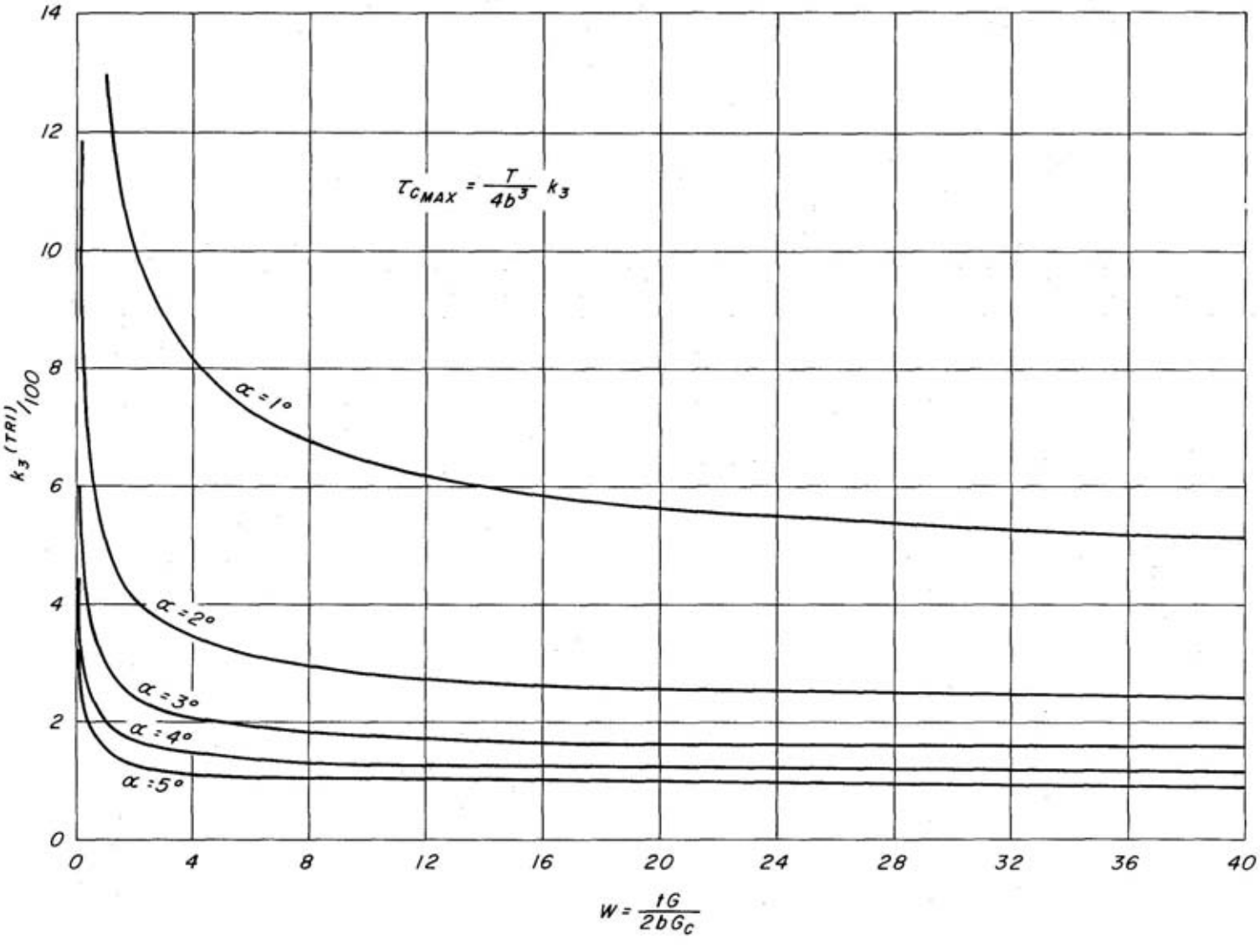

Figure 20.--Normalized maximum core shear stress for triangular sections. α = 1°, 2°, 3°, 4°, 5°.

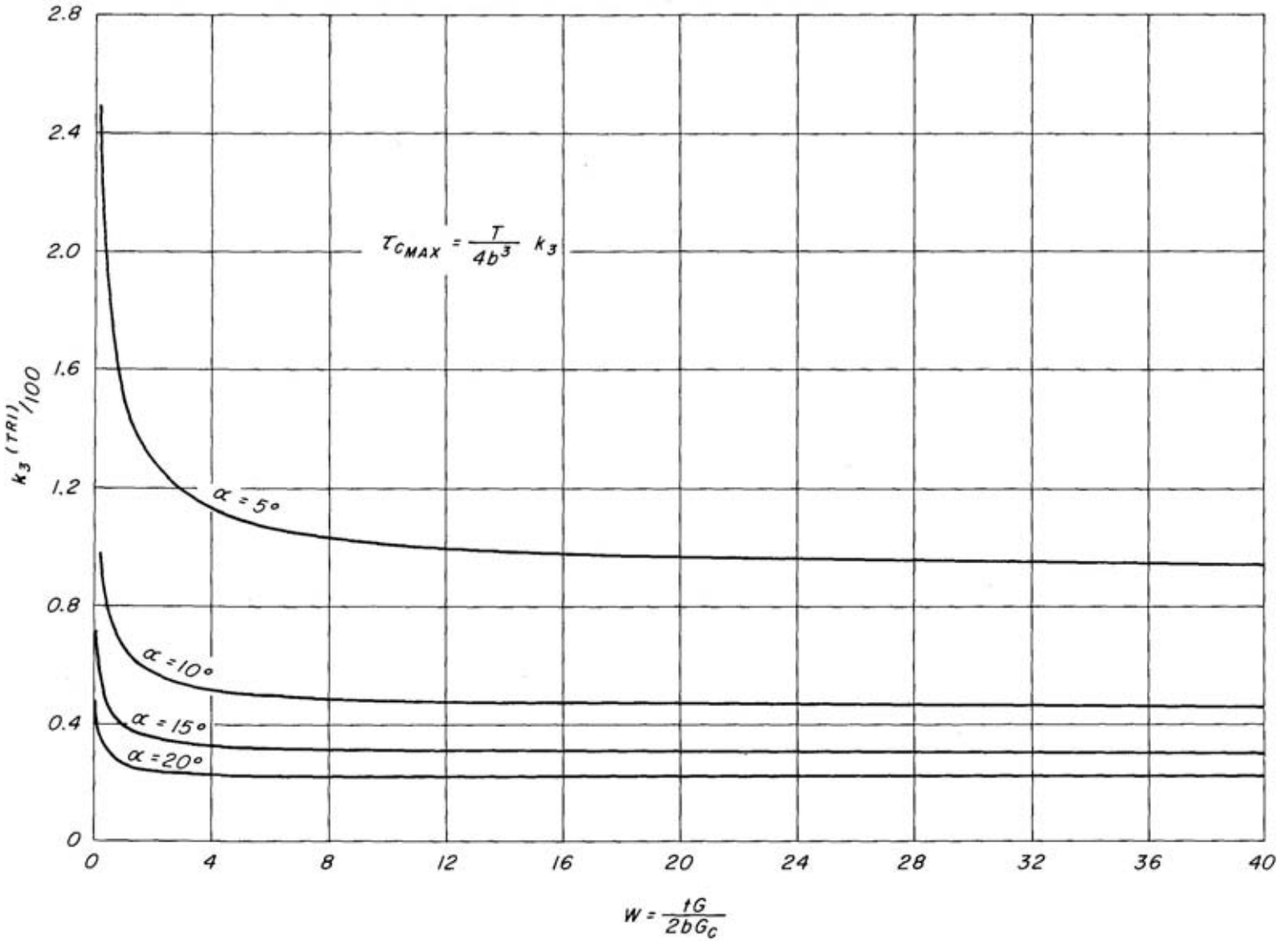

Figure 21.--Normalized maximum core shear stress for triangular sections. R = 5°, 10°, 15°, 20°.

M 140 396